Title

Excitation Functions of Bismuth

Author

Kelly, Elmer Lewis

Publication Date

2024-03-06

Bl. Harvey.

UCRL 1044
cy 2

KELLEY THESIS

UNIVERSITY OF CALIFORNIA

Radiation Laboratory

BERKELEY, CALIFORNIA

DISCLAIMER

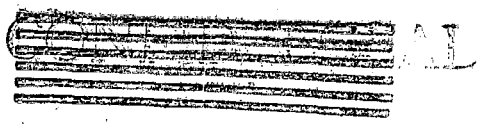

Excitation Functions of Bismuth

By

Elmer Lewis Kelly
B.S. (University of Virginia) 1941

DISSERTATION

Submitted in partial satisfaction of the requirements for the degree of

DOCTOR OF PHILOSOPHY

in

Physics

in the

GRADUATE DIVISION

of the

UNIVERSITY OF CALIFORNIA

Approved:

.....

.....

.....

Committee in Charge

Deposited in the University Library.....
Date Librarian

One of the many ways of studying nuclear properties is the determination of excitation functions. An excitation function is the absolute cross section for a particular nuclear reaction as a function of the energy of the bombarding particle which initiates the reaction. From these data one can obtain information on the binding energy of neutrons, protons, and alpha-particles in the nucleus. Perhaps more important is the fact that one can test nuclear models by comparing predicted excitation functions with the experimental data. As is usually the case in physics a great deal of experimental data on excitation functions must be accumulated before the broad outlines of a suitable theory will be clearly defined and as yet not nearly enough data has been taken. It seems that as the study of excitation functions progresses new details, sometimes unexpected, show up and in this way we are led to add more details to our models.

It was first pointed out by Bohr[1] that every nuclear process must be considered as a many-body problem. When a particle strikes a nucleus it cannot pass through without strong interaction with one or more of the nuclear particles; in fact, unless the nucleus is very light and the particle rather energetic, the particle will start interacting, and therefore losing energy, at the nuclear surface. This energy dissipation will continue as the particle penetrates the nucleus until the initial energy of the original particle is shared by all the particles of the system. This system consisting of the original nucleus and the incident particle is known as the "compound nucleus." This compound nucleus persists for a comparatively long time, i.e., until enough energy may "by accident" again be concentrated in one particle

to allow it to escape the nuclear force barrier, or until the energy is lost by nuclear radiation. Thus the nuclear collision may be described as two distinct processes: the formation of the compound nucleus and the decay of the compound nucleus. Under this assumption the theory of nuclear collisions is in most cases primarily a theory of the quasi-stationary states of the compound nucleus, and a theory of the transition from the compound states to states in which some particle of the compound nucleus is separated from the rest. Thus the cross section $\sigma(a,b)$ for a nuclear reaction in which a nucleus is bombarded with a particle a and a particle b is emitted may be expressed by $\sigma(a,b) = \sigma_a \eta_b$ where σ_a is the cross section for the compound nucleus formation and η_b is the relative probability that the particle b is emitted.

To obtain any quantitative results we must make some assumptions about the nuclear structure. For fast particles incident on heavy nuclei, which is the case for the experimental work described in this paper, the nucleus can be considered as a condensed phase of the neutron-proton system in the thermodynamical sense. The neutrons and protons are closely packed so that the nuclear volume is proportional to the mass number. By assuming a spherical form we can take a nuclear radius R equal to $r_o A^{1/3}$ where A is the mass number and r_o is of the order of 1.5×10^{-13} cm. We also assume the characteristic properties of the nucleus are retained even if the nucleus is highly excited. On the basis of these general ideas and assumptions Weisskopf[2] has derived specific equations for the compound nucleus cross sections and the relative emission probabilities for particle emission.

Three energy regions for the incident particle energy are dis-

tinguished by Weisskopf: region I where the energy is more than 1 or 2 Mev above the potential barrier; region II where the energy is less than 1 or 2 Mev above or below the barrier; and region III where the energy is more than 1 or 2 Mev below the barrier. The derived cross section equations for these regions are

$$\sigma_{a\alpha\ell} = \xi\ (2\ell + 1)\ \pi\lambda\!\!\!^{-2}_{a} \qquad \text{region I}$$

$$= \xi\ \frac{K_a}{K_o}\ (2\ell + 1)\ \pi\lambda\!\!\!^{-2}_{a}\ T_{a\ell}(\varepsilon_a) \qquad \text{region II}$$

$$= \xi\ (2\ell + 1)\ \pi\lambda\!\!\!^{-2}_{a}\ P_{a\ell} \qquad \text{region III}$$

$\underline{a}$ refers to the incident particle, $\underline{\ell}$ to its angular momentum and $\underline{\alpha}$ to the state of the initial nucleus. ξ is a pure number smaller than unity which goes to unity at high energies and is introduced to take care of transition regions. K_o is the wave number of the incident particle near the nuclear surface on the outside and K_a is the corresponding wave number near the nuclear surface on the inside. P_a is the well known exponential penetration factor for the barrier B_ℓ where B_ℓ includes both the Coulomb and the angular momentum effects. T_a is the barrier transmission coefficient and below the barrier is given in the W. K. B. approximation by

$$P_a \left(\frac{B_\ell - \varepsilon_a}{\varepsilon_a}\right)^{1/2}$$

where ε_a is the energy of the incident particle. From these equations one can calculate directly the cross sections for bombarding particles and this has been done by Weisskopf for protons and alphas incident on representative nuclei of atomic numbers from 20 to 90. Values are given for $r_o = 1.5 \times 10^{-13}$ cm^2 and $r_o = 1.3 \times 10^{-13}$ cm^2. No accurate

check on these calculations can be made since neither the "sticking factor" ξ nor the incident particle radius is numerically specified. However fairly accurate interpolation is possible and has been carried out for comparison with the experimental data given below. It should be noted here that in these calculations of Weisskopf he has neglected the region II equation completely and joined the solutions for regions I and III smoothly at the center of region II. This may explain the failure of the calculated values to fit the experimental data in this region.

The relative emission probability η_b for the compound nucleus is given by

$$\eta_b = \frac{f_b}{\sum f_c}$$

where the summation is taken over all particles c which can be emitted and the function f is the integral of the emission probability for b integrated from zero energy to the maximum energy b can have. On the assumption of an evaporation process from a highly degenerate Fermi-Dirac gas with a Maxwellian distribution of the evaporating particle energies, Weisskopf has calculated some typical f values which are shown in Fig. 1. It is clear from these values that only the neutron emission probabilities need be considered in computing the η_b values. One gets the following specific equations

$\sigma(p,n) = \sigma_p$ up to the threshold for the (p,2n) reaction

$\sigma(p,2n) = \sigma_p \left[1 - \left(1 + \frac{\Delta\varepsilon}{kT}\right) e^{-\Delta\varepsilon/kT}\right]$ between the (p,2n) threshold and the (p,3n) threshold.

Here kT corresponds to the nuclear temperature of the residual nucleus

[the value of kT one gets depends on the nuclear model used] and $\Delta\varepsilon$ is the excess of the incident proton energy over the (p,2n) threshold. Similar expressions hold for the corresponding deuteron and alpha induced reactions. One can also obtain an expression for $\sigma(p,3n)$ and consequently for $\sigma(p,2n)$ above the (p,3n) threshold. However the integration becomes tedious and the rather poor values resulting from the required approximations do not warrant the effort entailed.

In considering deuteron induced reactions one must also include the Oppenheimer-Phillips and stripping reactions. According to the results of Peaslee[3] the (d,p) and (d,n) reactions up to deuteron energies of 10 Mev or more are almost entirely due to the stripping process.

The experimental work reported in this paper has been confined to a single isotope at the heavy end of the periodic table, Bi^{209}. This isotope is convenient for a number of reasons: it is the only stable isotope of bismuth; it is readily available in high purity; it is easily evaporated to form thin uniform films; and most of the products formed by bombarding it with alphas, deuterons, or protons are alpha active which is convenient for the determination of absolute disintegration rates. Previous investigators[4-8] had available deuterons of energies up to 14 Mev and alphas up to 28 Mev. The present work has been done with 19 Mev deuterons, 38 Mev alphas, 390 Mev alphas, and 32 Mev protons. The method used is the well-known stacked foil technique with improved energy definition and beam current measurement. A stack of aluminum foils, each having a thin film of evaporated bismuth on one side was exposed to the accelerated particle beam. In some runs the stack was not thick enough to stop the beam and the beam was caught in

a Faraday cup, amplified, and fed into a recording milliameter; in others the stack was placed inside a large Faraday cup which was connected to a beam integrator of conventional type. The mean range of the beam was found by determining the amount of aluminum absorber required to reduce the beam intensity to one-half. The activity induced in the bismuth foils was counted by means of a parallel plate ionization chamber. Figs. 2, 9, and 12 give schematic diagrams of the apparatus used for the bombardments. Tables I, II, III, and IV and Figs. 5, 6, 11, and 14 give the final results, i.e., the cross sections for the various nuclear reactions as a function of the energy of the bombarding proton, deuteron, or alpha-particle.

Methods and Results

I. Experiments with the 60-inch cyclotron

In spite of the excellence of the work that had already been done with alphas and deuterons on bismuth,[4-8] the availability of the 19 Mev deuteron beam and the 38 Mev alpha beam of the 60-inch cyclotron with their higher energies made further work worthwhile. In addition to checking the (d,p) and the (d,n) reaction cross sections it seemed likely that the 19 Mev deuteron beam on bismuth would be able to produce the (d,2n) and (d,3n) reactions, enabling their cross sections to be determined. The (d,2n) reaction would be particularly interesting as it would produce the undiscovered isotope Po^{209}. The alpha beam on bismuth in addition to producing the well-known $Bi(\alpha,2n)At^{211}$ reaction[8] would probably produce the $(\alpha,3n)$ reaction and possibly in low yield the $(\alpha,4n)$ reaction. Both the latter reactions would result in new astatine isotopes and it was hoped one might be long-lived. Such an

astatine isotope would greatly facilitate the study of the chemical properties of astatine, which work was being done at that time[9] with the 7.5-hour At^{211}. The cross section for the (α,n) reaction was expected to be so strongly suppressed as to be unobservable.

Experimental Details

The aluminum foil used as backing for the evaporated bismuth, and for the energy determination absorbers, was punched on a die whose area was accurately measured. The dimensions of several foils were also measured with a traveling microscope. The areas of the various foils agreed to better than 3 parts in a thousand. Each backing foil, which was 0.001-inch thick, was thoroughly cleaned in CCl_4 and absolute alcohol, and weighed on an assay balance to the closest 0.01 mg. Next the foils were placed in a high vacuum chamber and bismuth evaporated onto them to the desired thickness. (Most runs were made with 1.0 to 1.5 mg cm^{-2} of bismuth.) The foils were then reweighed and the thickness of bismuth determined with an estimated accuracy of 1 part in 200 or better.

The raw beam of the 60-inch Crocker cyclotron had enough inhomogeneity in energy so that a better definition of the energy was required. This was obtained with a collimation system which consisted of the deflector channel of the cyclotron and the 1/8-inch slit shown in Fig. 2. Because of the fringing magnetic field of the cyclotron, this collimation system served as a velocity selector producing a beam of very homogeneous energy. Tests of energy versus deflector voltage showed a dependence of 0.04 Mev per kilovolt on the deflector. In practice the deflector voltage was held constant within 2 kilovolts

for the entire run. Since this collimation reduced the primary beam intensity by a factor of approximately one hundred (from 10^{-5} - 10^{-6} to 10^{-7} - 10^{-8} amp.) a sensitive beam current integrator was necessary. The current to the Faraday cup of Fig. 2 (10^{-7} to 10^{-8} amp.) was amplified to 1 milliampere by a modified version of the current amplifier described by Vance[10] and recorded on an Esterline Angus recording milliameter. The integrated beam current was found by planimetering the area under the trace. The trace of each run was planimetered by two people, and the agreement was 1 part in 200 or better. Allowance was made of the peculiar form of the Esterline Angus trace.

The range of the collimated beam was determined in a manner similar to that described by Wilson.[11] The foil wheel shown in Fig. 2 contained aluminum abosrbers differing in thickness by approximately 1 mg cm^{-2}. Each of these absorbers in turn was placed in the path of the beam, while the amount of beam current stopped and the amount transmitted were determined simultaneously by current amplifiers.[10] This gave the fraction of the total beam current transmitted for various thicknesses of aluminum absorber. From this data the mean beam range was at once determined. The position of the foil wheel could be changed by remote control, and since the stacked bismuth foils were contained in the wheel it was possible to determine the beam range, bombard the stacked bismuth foils, and redetermine the beam range without turning off the cyclotron. The range data for a typical run are plotted in Fig. 3. It will be noted that there was little change in the beam range during the run. The straggling of 1.1 percent compares favorably with the theoretical minimum of 0.9 percent given by

Livingston and Bethe.[12] The range in aluminum was converted to energy using the table of Smith.[13]

The activity induced in the bismuth films was followed by counting each sample in a parallel plate ionization chamber having a depth of 1.5 cm and filled with argon at a pressure of 1.7 atmospheres. The pulses from electron collection in the chamber were fed into a preamplifier and then into an amplifier whose time of rise was 0.2 microsecond. The amplified pulses were discriminated and counted on a 256 scaling circuit and mechanical register. The counter was checked against a standard alpha-particle source (a thin uranium sample electro-deposited on platinum) at the beginning and end of each counting period, and was found to remain constant to one percent over the entire period of 4 years during which these studies were made. The background was 1 to 2 counts per minute. The counting rate of the uranium alpha standard as a function of discriminator bias is shown in Fig. 4. The counting efficiency was 50 $\pm$ 1 percent at the operating bias of 14. This takes into account the absorption in the sample itself and the back-scattering from the support.

The possibility of error in the beam current measurements as a result of gas ionization or secondary electron emission was investigated. The space around the Faraday cup and the foil wheel was connected to the cyclotron tank during normal operation, as shown in Fig. 2. Since the pumping speed of the opening of the defining slits was small, a leak in this region could cause a substantial increase in pressure with a resulting increase in gas ionization along the path of the beam between the slits and the Faraday cup. Any selective collec-

tion of these gas ions would, of course, introduce an error. To test this effect, the pressure in the region of the Faraday cup was increased from 0.1 to approximately 10 microns of mercury, but no evidence of gas ionization was observed on the beam current meters. Hence this possible source of error must be ruled out. The effect of possible secondary emission of electrons is also ruled out. The fringing magnetic field of the cyclotron is 2500 gauss in the region where the Faraday cup was located. The resulting curvature in the path of any secondary electron formed by the beam striking the bottom of the Faraday cup would be more than sufficient to prevent the escape of the electron.

Bi(α,2n) and Bi(α,3n) Excitation Functions

At bombarding alpha energies below 29 Mev the only alpha-particle activity observed in the bombarded bismuth was that of At^{211}, which has a half-life of 7.5 hours. At higher bombarding alpha energies another alpha activity was observed after the 7.5-hour activity had died out. This was found to be due to Po^{210}. No other alpha activity was detected. This made the separation of activities very simple. Alpha counts 5 or 6 days after bombardment gave only the Po^{210} activity; correcting this for decay and subtracting from alpha counts made within 24 hours after bombardment, we obtained the activity resulting from At^{211}, which could then easily be extrapolated back to the time of the end of bombardment. This method of separating the activities was quick and accurate.* The question immediately arose, however, as to the

* This method neglects the 8.3-hour half-life for formation of the Po^{210} mentioned below, but the resulting error introduced is negligible in all cases.

origin of the Po^{210}. Careful investigation, which will be discussed in detail later, showed that essentially all the Po^{210} came from the Bi(α,3n) reaction producing At^{210} which in turn decays to Po^{210} by orbital electron capture, with a half-life of 8.3 hours.* Thus the At^{210} which had no alpha activity decayed to an alpha emitter which was readily counted on an absolute scale. The results of three runs were analyzed in this way and reduced to absolute cross section versus energy of the bombarding alphas. One run was made with bismuth films of 0.3 mg cm^{-2}, one with 1.5 mg cm^{-2}, and one with 2.0 mg cm^{-2}. When the results of the runs were first compared a dispersion of a few percent was found, which was felt to be outside the experimental error. After thorough checking, this dispersion was tentatively laid to the inaccuracy in the stopping power ratio of bismuth to aluminum, which had been extrapolated from the value for gold given by Bethe.[12] A subsequent experimental determination[14] of this stopping power ratio removed the apparent dispersion. The results of the three runs are shown in Fig. 5 and Table I.

Bi(d,p), Bi(d,n), Bi(d,2n) and Bi(d,3n) Excitation Functions

The activities resulting from deuterons on bismuth are more difficult to separate than those from alphas on bismuth. Early work has established the production of RaE(Bi^{210}) and Po^{210} from the Bi(d,p) and Bi(d,n) reactions.[4-7] Later work[15] indicates that the Bi(d,2n) reaction is not ordinarily observed and that the alpha activity at these

* The accuracy of this investigation does not exclude the possibility that a few percent of Po^{210} might have been produced by (α,dn), (α,p2n), or similar reactions.

energies, other than that due to the Bi(d,n) and Bi(d,p) reactions, is due to the Bi(d,3n) reaction which results in Po^{208} with a half-life of about 3 years.

For the separation of the Po^{210} with a 140-day half-life, the Po^{208} with a 3-year half-life, and the RaE, which goes by 5-day beta-decay to Po^{210}, the following procedure was adopted.* Each sample was alpha counted within several hours after bombardment and daily for a week; each sample was counted again after 2 months when all of the 5-day RaE had decayed into Po^{210}, and thereafter once every 3 months for a year. In order to determine the Po^{208} half-life, ten samples were analyzed by trial and error into 140-day Po^{210} and Po^{208}, such that when the Po^{210} activity was subtracted, the resulting activity fell on a straight line on semilog paper. The slope of this line gave the Po^{208} half-life. The result was 3.0 ± 0.2 years where the error given is based on internal consistency only. Each bombarded sample was then analyzed by the same method except that the resulting activity after Po^{210} subtraction was required to fit a straight line with a slope corresponding to a half-life of 3.0 years. This yielded the Po^{208} activity, which was extrapolated back to the time at the end of bombardment, and the total Po^{210} activity which was also extrapolated back to the time of the end of bombardment. Subtracting the extrapolated Po^{208} from the activity measured immediately after bombardment gave the Po^{210} due to the Bi(d,n) reaction. From the extrapolated total Po^{210} activity and the Po^{210} activity due to the Bi(d,n)

---

* It was not practical to use the difference in energy between the alphas of Po^{208} and Po^{210} to distinguish between the two because the difference is too small (5.298-5.14 Mev).

reaction, the amount of RaE was found. The amount of RaE was also found by the growth of the total alpha activity in the first week after bombardment. These two determinations of RaE agreed within one percent.

The Po^{208} activity as derived by this decay analysis was found to be produced below the calculated threshold for a (d,3n) reaction. Further close examination of the alpha activity in the energy region between 10 and 15 Mev showed a new alpha activity having an energy of 4.90 Mev. By means discussed in detail later this activity was identified as Po^{209}, formed by the previously unobserved (d,2n) reaction, with an estimated half-life of the order of 100 years. Due to the long half-life its presence did not affect the decay analysis for the RaE and the Po^{210}. However further analysis was required to distinguish the Po^{209} from the Po^{208}. Pulse analysis by A. Ghiorso of selected samples indicated the general shape of the Po^{209} yield curve which agreed very well with that expected from a (d,2n) reaction. The activity of the samples was followed for two years longer. These later data, corrected for the small amount of Po^{210} still present, were subjected to decay analysis by the method of least squares on the assumption that the corrected activity was due to 2.93-year[16] Po^{208} and 100-year Po^{209} only.

The results of two runs of deuterons on bismuth reduced to absolute cross section *versus* energy of the bombarding deuterons are shown in Fig. 6 and Table II.

ASTATINE^{210}

Bismuth bombarded with alpha-particles of 37 Mev energy yields the 7.5-hour alpha activity of At^{211} and the 140-day alpha activity of Po^{210}, as was mentioned above; in addition, there is an easily dis-

tinguishable gamma-ray activity. The Po^{210} alpha activity was found to decrease with decreasing energy of the bombarding alphas, disappearing with alpha energies below 29 Mev (see Fig. 5). The gamma activity likewise disappeared with bombarding alpha energies below 29 Mev. The gamma activity was found to follow the At^{211} alpha activity quantitatively through a chemical separation and through a vacuum distillation over to a cold platinum plate.[9] In the separated astatine fraction Po^{210} alpha activity could be observed after the relatively short-lived At^{211} alpha activity had decayed out. These results suggested that Po^{210} was formed as a decay product of a new isotope of astatine, probably by capture of an orbital electron of At^{210} which had been formed by an $(\alpha,3n)$ reaction on bismuth.

In order to study the formation of the Po^{210} more carefully, a G-M counter was constructed having an optimum x-ray counting efficiency in the region of the K x-rays of polonium. This counter was a Chicago type, having a cylindrical aluminum wall 0.25 mm thick lined with tin foil 0.08 mm thick. The counter was filled with argon plus 10 percent of alcohol to a pressure of 10 cm of mercury.

Two samples of astatine were studied with this G-M counter and with the alpha counter. Sample A was prepared by bombarding thin bismuth with alphas of 25 Mev energy and then extracting the astatine by a vacuum distillation over to a cold platinum plate; sample B was prepared in the same way except that the bombarding alphas had an energy of 37 Mev rather than 25 Mev. Absorption in lead indicated that a gamma-ray of 1.0 Mev energy was present in sample B but was not present in sample A, as is shown in Fig. 7. This gamma-ray was found

to decay with a half-life of 8.3 hours. Absorption in aluminum showed that some 0.9 Mev electrons accompanied the gamma-rays; these were in all probability conversion electrons of the 1.0 Mev gamma-rays. Absorption in platinum and tungsten revealed that both samples emitted x-rays showing the absorption properties to be expected for the K lines of polonium. The ratio of the K x-ray counting rate to the alpha counting rate was 10 to 14 times as large in sample B as in sample A. In sample A the half-life of the K x-rays was 7.5 hours; in sample B the half-life of the K x-rays was slightly more than 8 hours. Po^{210} was found in sample B but not in sample A. Clearly, sample B contained a new isotope of astatine, most if not all of which decayed into Po^{210} with the emission of K x-rays and gamma-rays.

The existence of At^{210} and its decay by orbital electron capture to Po^{210} being thus established, the question arises as to whether all the Po^{210} found in our alpha bombardment was produced through the decay of At^{210} or whether some was formed directly by a Bi(α,2np) reaction. This question could be settled in several ways. The method chosen consisted, in principle, in dividing a thin bombarded bismuth foil into two equal parts and extracting all the astatine from one part immediately after bombardment. A week later only the Po^{210} activities were left and were readily determined by alpha counting each sample. If all the Po^{210} formed is a duaghter of At^{210}, the unextracted sample and the extracted astatine sample must each have the same activity. On the other hand, if some of the Po^{210} is formed directly at bombardment then the unextracted sample must have a greater activity than the extracted astatine sample.

In practice this procedure requires enough time so that an extrapolation must be made back to the time of the middle of the bombardment. In order to make this extrapolation the procedure was repeated allowing various time intervals between the bombardment and the astatine extraction. To eliminate the effect of unequal division of the bombarded bismuth foil and variation of the extraction yield, the amount of At^{211} alpha activity in each sample was used for normalization. The ratio of the Po^{210} resulting from the decay of the extracted astatine to the total Po^{210} formed plotted as a function of extraction time is shown in Fig. 8. The decay is seen to agree quite well with the 8.3-hour half-life found for the gamma-rays. The zero time intercept (the time of the middle of the 50-minute bombardment) shows that within the experimental error all the Po^{210} was formed by the decay of the At^{210}.

Clearly, the results shown in Fig. 8 are valid only if the astatine extractions are free from polonium contamination. For this reason the extraction process[9] employed here will be described briefly. When an alpha-bombarded sample of bismuth on aluminum is heated in the presence of silver in an evacuated glass vessel, the astatine vapor is selectively adsorbed by the silver. Careful tests have shown that after 10 minutes at 310° C more than 85 percent of the astatine alpha activity was collected on the silver foil. Under the same conditions, using a bombarded bismuth sample from which all the astatine had decayed out, only 0.07 percent of the polonium alpha activity present in the bismuth appeared on the silver foil. For this astatine separation method neither the temperature nor the heating time was very critical; however, the bismuth had to be melted (273° C or more), and the polonium

contamination increased slowly with increasing temperature.

If there were any appreciable alpha-branching in the decay of At^{210}, as there is in At^{211}, one should see evidence of this alpha activity and evidence of the decay product, which would be Bi^{206} with a 6.4-day half-life. Examination of extracted astatine in the 48-channel pulse analyser[17] showed no alpha activity other than that of At^{211} and Po^{210}. If the branching ratio had been 1 part in 100 or larger the resulting alpha activity could have been observed provided it had an energy different from that of the At^{211} and the Po^{210}. Examination of the astatine extracted from a thick bismuth target bombarded with 200 microampere hours of alpha-particles having an energy of 37 Mev showed no evidence of 6.4-day activity. If 1 part in 10^3 of the At^{210} had decayed by alpha emission, the 6.4-day Bi^{206} should have been observed.

POLONIUM^{209}

Bismuth bombarded with 19 Mev deuterons yields in addition to RaE, Po^{210}, and Po^{208}, another alpha activity of 4.90 Mev energy. This activity follows the Po^{210} and Po^{208} quantitatively through chemical separation and electro-deposition and must therefore be an isotope of polonium. The 4.90 Mev alpha activity appears with deuteron energies of about 8 Mev, increases to a maximum at about 15 Mev and then decreases as the deuteron energy increases. This yield is just what one would expect from a (d,2n) reaction. Since this activity is due to an isotope of polonium and the Bi(d,p), Bi(d,n), and Bi(d,3n) reactions are known to produce activities different from this, one must conclude that this new activity is due to the missing isotope Po^{209} produced by

the previously unobserved Bi(d,2n) reaction. This assignment is confirmed by the proton bombardment of bismuth described below. The low yield of the new activity indicates a relatively long half-life compared to the 3-year Po^{208}; the actual decay of the activity is as yet less than the observational errors of counting. This is due in part to the presence of other activities and in part to the limited period of observation (four years). The K-capture branching has been estimated[18] to be at most 1 part in 10. If we make assumptions about the cross section for the formation of Po^{209} we can get an estimate of the half-life. On the basis of such assumptions (discussed in detail later) and on the assumption of no K-capture at all, using yield data of both deuteron and proton bombardments, the half-life is estimated to be about 100 years (this differs somewhat from an earlier estimate of 200 years based on preliminary deuteron bombardment data alone). This value is expected to be within a factor of two of the true half-life.

As can be seen from the data of the proton bombardments described later a large sample of Po^{209} free of lighter polonium isotopes could be produced in the 60-inch cyclotron proton beam. It would be contaminated only by Po^{210}, its activity being about half that of the Po^{209}. With such a sample one could measure the K-capture branching, and in about five years one could also obtain a fair value for the half-life.

II. Experiments with the 184-inch cyclotron

When the 184-inch synchro-cyclotron began to operate,[19,20] the possibility of extending the excitation function work on bismuth was of course considered. There were many difficulties involved, the most formidable one being the separation and identification of the many

reactions that would certainly occur at these high energies (190 Mev deuterons and 390 Mev alphas). This was especially true since the product isotopes of most of the expected reactions were as yet unidentified. However, one reaction that would certainly occur, $Bi^{209}(\alpha,2n)At^{211}$, produces an isotope that is easily distinguishable due to the two alpha energies resulting from its decay and its 7.5-hour half-life.* In the present work the excitation function, or rather the yield function, for this reaction has been measured up to alpha energies of 390 Mev.

Experimental Details

The use of the stacked foil technique excludes the possibility of intercepting the circulating beam directly in the 184-inch cyclotron since there is no assurance that all the particles are intercepted by the first foil and spend their full range in the foil stack. The external alpha beam of the 184-inch is too small (10^{-11} amp.) to produce sufficient activity. There remains the possibility of intercepting the electrostatically deflected beam[21] internally. This method proved to be feasible and was used in the present work.

The general arrangement of the apparatus during bombardment is shown in Fig. 9. The stack of evaporated bismuth foils and suitable aluminum absorbers was mounted in an insulated 1/4-inch wall aluminum tube behind a grounded 3/4-inch copper beam defining plate. For electrostatic shielding the entire assembly was covered by a grounded copper house having a 1 mil aluminum window in front of the beam de-

* At^{211} decays with a 7.5-hour half-life, 40 percent by emission of 5.9 Mev alphas and 60 percent by K-capture to AcC' which has a half-life of 0.52 second and decays by emission of 7.4 Mev alphas.

fining plate. Baffled openings were provided to prevent pressure build-up inside the shielding. There was 1 cm or more clearance to the foil stack and holder at all points. 1 cm is the radius of a 3.8 Mev electron in the 184-inch magnetic field at this point; thus secondary electron emission would not affect the beam monitoring. Assuming that the pressure inside the shield was the same as in the cyclotron tank, the ionization current was approximately 10^{-5} ion pairs per α, and thus negligible. The beam current (approximately $1/2 \times 10^{-8}$ amp.), was integrated by the regular 184-inch beam integrater, which consisted of an amplifier and a watt-hour meter. In order to get as much activity as possible the foil area was large, 31 cm^2, and the bismuth about 3 mg/cm^2 thick; thicker foils would have necessitated chemical extraction with the attendant uncertainty in yield and delay in getting the samples counted.

The method of counting the At^{211} was in principle quite simple. All alpha pulses above 6.5 Mev were counted in a grid ionization chamber and the half-life followed to ascertain that it was 7.5-hour activity. It was assumed that the chance of an isotope having a 7.5-hour half-life and alphas of energy greater than 6.5 Mev was vanishingly small. In order to find the greatest permissible thickness of bismuth, foils of various thicknesses were bombarded in the 60-inch cyclotron and counted in the grid chamber. It was found that separation of the two At^{211} alpha ranges was just discernible in samples 4 mg/cm^2 thick. See Fig. 10. To be safe the run was made with 3 mg/cm^2 samples. During the actual counting of the 184-inch samples the counter was periodically calibrated by counting a sample of pure At^{211} in a 3 mg/cm^2 bismuth

foil. The drift was only a few percent and was easily corrected for.

The beam current monitoring system was considered to be somewhat unreliable due to the possibility of pickup from the rf voltage on the cyclotron dee and from the electrostatic deflector system. For this reason it was decided to determine the absolute cross section scale by comparing the 184-inch Bi(α,2n) yield curve with the one obtained from the 60-inch cyclotron. A little consideration shows that if the (α,2n) yield is plotted as a function of absorber in the beam, the area under the curve is independent of the energy distribution in the primary beam. Thus in spite of the fact that the 184-inch beam has an unknown energy distribution, the 184-inch curve can be normalized by comparison with the 60-inch curve. When this was done the results by this method and by beam current monitoring differed by 7 percent, which under the circumstances is quite satisfactory. The curve matching method however is considered the more reliable and has been used in preparing the final data. By matching the maxima of the two curves one also obtains a fiducial point on the energy scale of the 184-inch curve. The results obtained in this way are shown in Table III and Fig. 11. Strictly speaking this is just an absolute yield curve for the 184-inch electrostatically deflected alpha beam. To obtain an excitation curve one would need to know the energy distribution in the beam, the nuclear absorption of the alpha beam, and the number of secondary alphas produced in each energy interval above 18 Mev. This is discussed in detail below.

It might be mentioned in passing that a preliminary determination of the excitation curve of the $Bi(p,2n)Po^{208}$ reaction for proton ener-

gies up to about 35 Mev was made with the 184-inch cyclotron. The bismuth foils were exposed individually as interceptor targets at different radii. Each bismuth on aluminum foil was backed by a thin graphite foil of the same size and the activity of the $C^{12}(p,pn)C^{11}$ reaction was used for monitoring. The proton energy for each sample was computed on the basis of magnetic field measurements of the cyclotron, radius of the target, and the assumption that the proton orbits were central and non-oscillatory. The results compare satisfactorily with the more accurate data later obtained with the linear accelerator protons. Thus the experiment indicates that this technique can be used satisfactorily where the experimental conditions make it necessary or convenient.

III. Experiments with the 32 Mev proton linear accelerator

Successful operation of the proton linear accelerator at this laboratory[22] made possible the study of proton induced reactions in heavy elements. Considerations of the possible proton induced reactions in bismuth and the resultant activities indicated that the beam size (2×10^{-8} amperes) was just adequate. The (p,2n), (p,3n), and (p,4n) reaction activities could probably be seen with an hour or two bombardment of thin bismuth foils (1 or 2 mg/cm^2); the (p,n) reaction would require thicker foils, longer bombardment, or both, due to the long half-life of the resulting activity. The cross section for the (p,γ) reaction was expected to be so low as to escape detection entirely. Thus most of the possible reactions could be studied by a short bombardment of the usual type of foil stack. The separation of the three main activities could easily be done by decay analysis since

the half-lives involved are 3 years, 5.7 hours, and 9 days. To follow the (p,n) reaction it was decided to make a stack consisting entirely of thick bismuth foils and bombard it for 10 to 20 hours. The polonium would be extracted chemically from each foil and electro-deposited to give a thin sample. This thin sample could then be pulse analyzed to separate the alpha activities of the various polonium isotopes present.

Experimental Details

The foil stacks used in runs 1 and 2 were prepared by evaporating bismuth onto aluminum foils in the same manner as described previously. Run 1 had approximately 1.5 mg/cm^2 bismuth layers with aluminum absorbers in between while run 2 had alternate layers of 1.5 and 6 mg/cm^2 bismuth interspersed with aluminum absorbers. This latter arrangement gave an accurate check on the self absorption correction which was applied to all foils. The stack for run 3 consisted of bismuth foils alone ranging from 20 mg/cm^2 to 50 mg/cm^2. These foils were prepared by evaporating the bismuth onto dural and then peeling the dural from the bismuth; this bismuth foil was then punched into 1-inch diameter discs on an accurately ground die punch. It was found that such a stack of thick bismuth foils melted when bombarded in a vacuum by the 32 Mev proton beam (2×10^{-8} amp.). Hence run 3 using these foils was made by bringing the beam out through an aluminum window and bombarding the foil stack in air. The foils were spaced 1/32-inch apart and cooled by a fan. (Even so some discoloration of the foils due to heating was observed.) The experimental arrangement during bombardment is shown in Fig. 12.

At the time of the first run no convenient apparatus for measuring

the beam energy existed and so the energy scale for this run has been obtained by matching it to run 2. The energy of the beam was measured at the time of the second run by the use of aluminum absorber wheels that could be varied by remote control. Some difficulty was introduced by the fact that there was no beam monitor in front of the aluminum absorber.* Consequently one had to depend on the beam remaining steady while the current to the Faraday cup was measured first with no absorbers, then with absorbers, and again without absorbers. The results appear to be fairly consistent and are shown in Fig. 13. The mean beam range was found to be 1240 mg cm^{-2} aluminum, corresponding to 31.3 Mev, and the extrapolated range 1284 mg cm^{-2} aluminum corresponding to 31.8 Mev. Perhaps it should be noted here that the energy of the proton beam varied somewhat with the plate voltage of the oscillators and that minor tuning of the first and last drift tubes could be effected by mechanical adjustment from outside the tank. Likewise the drift tube tuning could change because of mechanical motion due to heating. These effects make it impossible to preset the machine to the same beam energy each run and consequently the beam energy varied slightly from one run to the next. In run 3 the foil stack could not be placed in the Faraday cup and so it was not possible to integrate the beam accurately. In addition, since the run consisted of two 10-hour bombardments a week apart, accurate monitoring of the beam energy would have been very time consuming. Therefore both the energy and cross section scale of run 3 have been matched to that of run 2. The close match of the (p,2n) curves shows that the energy drift and

* The flux density of the beam is so great as to virtually "short circuit" any ordinary ionization chamber.

straggling was not appreciably more in run 3, than it was in run 2. As a further check a stack of bismuth foils was bombarded in the 60-inch cyclotron where the beam current and energy could be accurately measured. The resulting activity yield curve of course did not extend far above the threshold but was sufficient to compare with the corresponding data from the other runs. The agreement was quite good, indicating that the proton beam energy determination of run 2 was correct to within 0.3 Mev and that run 3 had an energy spread of approximately $\pm$ 0.4 Mev at 32 Mev. The foils of runs 1 and 2 were counted in the shallow ionization chamber described previously. The observable activities had half-lives of 3 years, 5.7 hours, and 9 days resulting respectively from the reactions $Bi(p,2n)Po^{208}$, $Bi(p,3n)Po^{207}$, and $Bi(p,4n)Po^{206}$. By following the total activity in each foil the amount due to each of these reactions was easily separated by decay analysis. Since the Po^{207} has an alpha branching ratio of approximately 10^{-4} its activity was a small fraction of the total, and since the 5.7-hour half-life prevented long counting times, the determination of the amount of the Po^{207} activity is not as accurate as one would have liked. There was no corresponding difficulty with the Po^{208} or the Po^{206}.

The foils of run 3 at the end of the bombardment had too much Geiger activity for safe handling and so were not counted until a week later. A careful count in the shallow ionization chamber gave a total activity thick target yield curve. In the region of the $Bi(p,2n)Po^{208}$ maximum yield there was no other appreciable activity and hence this part of the curve of run 3 could properly be matched to the $Bi(p,2n)Po^{208}$ yield curve of run 2 to obtain an absolute yield scale and a fiducial

point on the energy scale for run 3. Next the polonium of every second foil was extracted chemcially and thin samples of most of these prepared by electro-deposition or by vacuum distillation onto platinum foil. These prepared thin polonium samples were then pulse analyzed in the 48-channel analyser of A. Ghiorso to separate the Po^{208} and Po^{209} activities. Surprisingly Po^{210} activity was found in an amount comparable to the Po^{209} activity. This corresponded to a cross section of nearly a millibarn at the peak of the Po^{210} curve and seemed rather too high for a (p,γ) reaction in competition with a (p,n) reaction. However further investigation, described below, indicated that essentially all of the Po^{210} must have been produced by the (p,γ) reaction. The results of runs 1, 2, and 3 could now be combined to give alpha activity yield curves for the (p,γ), (p,n), $(p,2n)$, $(p,3n)$, and $(p,4n)$ reactions on Bi^{209}. To reduce these data to excitation functions one needs the half-life and alpha branching ratio for each of the polonium isotopes involved. For Po^{210} and Po^{208} the half-lives are 138 days and 2.93 years respectively and the branching ratios 100 percent. For Po^{207} and Po^{206} the half-lives are 5.7 hours and 9 days respectively; the alpha branching ratios have been taken to be 1.4×10^{-4} and 4×10^{-2} from yield considerations as described below, which is in good agreement with the ratios of 10^{-4} and 10^{-1}, previously reported.[15] For Po^{209} the branching ratio has been estimated to be greater than 0.9[18] while the half-life is estimated to be about 100 years. Using the half-lives 138 days, 100 years, 2.93 years, 5.7 hours and 9 days and the alpha branching ratios 1.00, 1.00, 1.00, 1.4×10^{-4} and 4×10^{-2} for Po^{210} to Po^{206} respectively the yield data has been reduced to

excitation functions. The results of runs 1, 2, and 3 are given in Table IV and Fig. 14.

The unexpectedly high yield of Po^{210} suggested that some reactions other than Bi(p,γ) might be contributing. Bi^{210} could be produced by the following reactions: $Bi^{209}(n,\gamma)Bi^{210}$ or $Bi^{209}(d,p)Bi^{210}$ followed by 5-day beta decay to Po^{210}; $Bi^{209}(d,n)Po^{210}$; or $Bi^{209}(\alpha,3n)At^{210}$ followed by 8.3 hours K-capture to Po^{210}. All but one of these involve a decay subsequent to the initial reaction but this cannot be ruled out for run 3, since this run consisted of two bombardments 7 days apart and the samples were not counted until 9 days after the second bombardment. Let us consider the alpha and deuteron reactions first. If the deuterons came from the linear accelerator their energy would be limited by the steering magnet (see Fig. 12) to approximately 16 Mev and a corresponding range of 220 mg cm^{-2} Al; likewise alphas from the accelerator would be limited to 32 Mev and a corresponding range of 110 mg cm^{-2} Al. Hence these alphas or deuterons could not reach into the foil stack beyond the equivalent of a proton energy of 29 Mev (a range of 1300 - 200 mg cm^{-2} Al). This rules out alphas or deuterons from the accelerator since the Po^{210} was observed throughout the foil stack and showed a peak at about 15 Mev. These reactions might also be due to secondary alphas or deuterons produced in the foil stack by the proton beam. However, in the 184-inch bombardment described above, 300 to 390 Mev alphas produced a yield of At^{211} of only 0.2 millibarn; even if this is all attributed to secondary alphas it is a factor of two or more too small and one would certainly not have as many secondary alphas of 30 Mev or more from 32 Mev protons on bismuth as from 350

Mev alphas on aluminum. Secondary deuterons might be formed in the stack from neutron pickup by protons of the primary beam. If one assumes all the Po^{210} to be formed by deuterons from this process a pickup cross section of about 10 barns results which is three times as large as the bismuth geometrical cross section. We consider finally the possibility of a $Bi^{209}(n,\gamma)Po^{210}$ reaction. If the neutrons come from outside the foil stack the Po^{210} yield should be independent of position in the stack which is certainly not the case for the observed Po^{210} yield. If the neutrons are produced within the stack and have an energy of 1 or 2 Mev one would expect the highest yield and hence the most Po^{210} at the high energy end of the stack where the compound nucleus is evaporating off the most neutrons. In addition the bismuth capture cross section for 1 Mev neutrons is only 3 millibarns requiring a neutron flux of about 1/5 that of the proton flux which is too high for the solid angle involved. If the neutrons responsible for the Po^{210} are produced within the stack and are thermal one would expect a rather uniform Po^{210} yield throughout the stack; also the capture cross section is only 15 millibarns requiring a thermal neutron flux of about 1/20 of the proton flux which is unlikely in view of the losses in thermalizing within the stack. It should be remembered that the foils were separated for air cooling which greatly increased the chance of a neutron escaping before becoming thermal.

The possibility of the Po^{210} arising from impurities is most unlikely. Any Po^{210} present in the bismuth before the bombardment would have given a uniform yield and in addition would most certainly have long since decayed out. Half-life considerations also rule out any

other known polonium as a contaminant. Lead as a contaminant would have been very slight since the bismuth used was of high purity and alphas would be required to produce the Po^{210} from lead which rules this out. Lighter contaminants need not be considered. Bi^{209} is the only stable isotope of bismuth which rules out the possibility of a $Bi^{210}(p,n)Po^{210}$ or a $Bi^{211}(p,2n)Po^{210}$ reaction. As a final check on the origin of the Po^{210} observed, a stack of bismuth on aluminum foils was bombarded in the 60-inch cyclotron and the resulting activity examined. The bombardment was made with the apparatus shown in Fig. 2 with the addition of a flexible joint and a 1.6 mg cm^{-2} Al window 15 inches in front of the foil stack. This window changed the accelerated H_2^+ ions into H+ ions or protons and the fringing magnet field of the cyclotron separated the proton beam from any deuteron or alpha contamination. In practice the position of the H_2^+ beam and the proton beam were separated by 1 inch at the foil stack collimator location; since a 1/8-inch collimating slot was used this separation was quite adequate. When the apparatus was lined up and the proton beam centered on the defining slits the current to the Faraday cup dropped by more than a factor of 10^3 when the 1.6 mg cm^{-2} Al window was removed. Thus one felt the proton beam used was essentially free from deuterons or alphas. The activity of the bombarded samples was followed very closely for signs of growth; none was found. This ruled out all reactions from alphas, deuterons, or neutrons. The only reaction that does not involve a subsequent decay to Po^{210} is the (d,n) but by Fig. 6 one can see that the (d,n) is accompanied by the (d,p) reaction hence the absence of the (d,p) requires the absence of the (d,n) reaction. As fur-

ther confirmation, the ratio of Po^{210} to Po^{209} of four samples of this run analyzed by A. Ghiorso agreed within a few percent with the corresponding ratios from run 3. One must conclude therefore that the ? $Bi(p,d)Po^{210}$ cross section has been correctly assigned and the high observed values are real. The theoretical implications of this are discussed below.

Discussion

The interpretation of the Bi(α,2n) and the Bi(α,3n) reactions produced in the 60-inch cyclotron can be made in a simple semi-empirical way. Let us consider first the cross section σ_α for the formation of the compound nucleus. Interpolating in the table of σ_α of Weisskopf[2] we obtain cross sections for bismuth for two values of the barrier height, 26.61 Mev and 23.06 Mev corresponding to $r_o = 1.3 \times 10^{-13}$ cm and 1.5×10^{-13} cm. These are shown by the solid lines in Fig. 15. If we sum the observed (α,2n) and (α,3n) cross sections we find passable agreement with the calculated σ_α for alpha energies above 25 Mev. This is taken to mean that in this region all other competing processes have comparatively small cross sections. Below alpha energies of 25 Mev the observed total cross section falls well below the value expected from the calculated σ_α. This indicates another reaction has an appreciable relative cross section below 25 Mev. It is reasonable to assume this to be the Bi(α,n) reaction which would produce At^{212}. An alpha activity of 0.25-second half-life has been produced by alphas on bismuth in this energy range and tentatively ascribed to At^{212} but the excitation function has not yet been determined.[23] Until this function has been measured it is impossible to check the theoretical σ_α in this region.

We can however get a value of r_o for bismuth. To do this we interpolate between the solid curves of Fig. 15 for a value of r_o that gives the best fit to the total observed cross section in the region between 30 Mev and 36 Mev (above 36 Mev the unobserved Bi(α,4n) reaction may begin to appear and below 30 Mev we approach region II where the calculations may be somewhat doubtful). This gives $r_o = 1.43 \times 10^{-13}$ cm^2. Using this value and continuing our interpolation of σ_α to lower alpha energies we obtain the dotted line shown in Fig. 15. It should be noted that the total observed cross section rises above this calculated curve in the region from 23 Mev to 28 Mev. Since this is just region II of Weisskopf where his calculations have been approximated by using the equations of regions I and III it is possible that a more accurate calculation would give a better fit. In any case this discrepancy casts doubt on the calculated σ_α in this region and consequently on any estimates of $\sigma_{\alpha,n}$ derived from the calculated σ_α.

In attempting to interpret the Bi(α,2n) yield curve of the 390 Mev alpha bombardment the effect of the energy distribution in the alpha beam must be considered. If one assumes this distribution to be Gaussian and adjusts the mean energy and energy spread of the beam to obtain the best fit to the excitation function obtained from the 38 Mev alpha bombardment, one finds fair agreement in the overlapping region. The best fit gives a mean alpha beam range of 9.40 gm cm^{-2} aluminum with a half-width at half maximum of 0.13 gm cm^{-2}. This corresponds to a mean energy of 388 Mev with a 3 Mev half-width at half maximum. If one computes the theoretical straggling of a 400 Mev alpha beam by extrapolation from data of Livingston and Bethe[12] one finds approximately 1.3

Mev. As one goes to the higher energy part of the yield curve the beam energy distribution becomes unimportant and the effect of nuclear absorption and secondary alphas must be considered. The foil stack was largely aluminum absorbers. The geometrical cross section for aluminum is $\pi R^2 = \pi(1.5 \times 10^{-13} \times 3)^2 = 0.6$ barn. If we assume that the cross section for nuclear absorption is equal to the geometrical cross section we find that the nuclear absorption is

$$\frac{10}{27} \times 0.6 \times 10^{+24} \times 0.6 \times 10^{-24} = \frac{3.6}{27} = 13 \text{ percent.}$$

By this calculation the yield curve is approximately 13 percent too high at 390 Mev due to nuclear absorption. In estimating the effect of secondary alphas we will consider only the highest energy region where the observed cross section is lowest and consequently most susceptible to error from this source. We assume rather arbitrarily the cross section for secondary alpha production to be the geometrical cross section and these alphas to have an energy of 25 Mev. Since the bismuth foils were separated in this region by approximately 1 gm cm^{-2} aluminum absorber the only secondary alphas that would be effective would be those produced in the aluminum just preceding the bismuth, about 20 mg cm^{-2}. This gives a cross section for At^{211} produced by these secondary alphas of 5×10^{-5} barn. If one looks at Fig. 11 one is tempted therefore to say that the difference in cross section between the highest energy point and the next point, which is approximately 5×10^{-5} barn, is real and due entirely to the effect of secondary alphas; at least this difference is of the right order of magnitude to be due to secondary alphas.

The half-life of Po^{209} given above has been estimated on the basis of yield considerations alone, with the assumption of no K-capture. The principle of the estimation is simple; one adjusts the half-life of the Po^{209} so that the total observed cross section for all reactions agrees best with the calculated cross section for the compound nucleus. However, in the case of the deuteron induced reaction at least, the theory is rather complex and unsatisfactory. According to Peaslee[3] our observed cross sections for the (d,p) and the (d,n) reactions on bismuth are fairly well accounted for on the basis of a stripping theory in which no compound nucleus is formed. These reactions have, therefore, not been included; the remaining (d,2n) and (d,3n) cross sections have been summed and compared with the calculated compound nucleus cross section for deuterons on bismuth derived from Weisskopf's table.[2] The results are shown in Fig. 16 for a Po^{209} half-life of 50 years, of 100 years, and of 150 years. There is certainly no agreement of the theory with any of the three half-lives used. However, the general shape of the curve corresponding to 150 years is perhaps the nearest to the shape given by the theory. If the (d,p) and (d,n) cross sections are included there is still no agreement with theory but the general shape is altered somewhat and the value of 100 years appears to give the best shape. This is all one can deduce about the Bi^{209} half-life from the deuteron data on the basis of these calculated cross sections.

The data of the proton induced reactions present a more encouraging picture. The observed cross sections for the (p,n) and the (p,2n) have been summed and compared with theory; the results for a Po^{209}

half-life of 50 years, 75 years, and of 100 years are shown in Fig. 17. Here the agreement with all three is good. If we interpolate to obtain theoretical values for $r_o = 1.43 \times 10^{-13}$ cm, we find the agreement is excellent in the region where the (p,n) cross section is relatively small; the agreement is quite good in the region where the (p,n) reaction is relatively large if we choose the Po^{209} half-life to be 50 years. This fit is unfortunately sensitive to the energy value assigned to the experimental data. If we assume the determination of the mean range of the proton beam to have been too low by 15 mg cm^{-2} of aluminum (this corresponds to an error of 0.2 Mev at 32 Mev which is a reasonable error) then the experimental points shown in Fig. 17 are shifted and one gets the results shown in Fig. 18. In Fig. 18 the fit for the 75-year half-life is at least as good as the fit in Fig. 17 for the 50-year half-life. Thus even if we assume the calculated σ_p, shown as the dashed line, to be correct, we cannot from the proton data be sure of the Po^{209} half-life to any better than about a factor of two. We have considered the indications obtained from both the deuteron and proton data and somewhat arbitrarily chosen the value of 100 years with the expectation that it is probably within a factor of two of the true value. This round number of 100 years has been used in the cross sections for Po^{209} given in the tables and graphs of this paper; when in the future this half-life is accurately determined these Bi(d,2n) and Bi(p,n) cross section values should be changed accordingly.

The satisfactory agreement between the experimental and theoretical values for the (p,n) and (p,2n) reactions on bismuth has encouraged us to use the same method for determining the K-branching ratios for

Po^{207} and Po^{206}, which are produced by the (p,3n) and (p,4n) reactions on bismuth. The total observed cross section for all the proton induced reactions is compared with the calculated values for the compound nucleus. By adjusting the K-branching ratios of the Po^{207} and Po^{206} an excellent fit is obtained as shown in Fig. 19 for alpha branching ratios of 1.4×10^{-4} and 4×10^{-2} respectively. As mentioned above this is in good agreement with the previously reported values[14] of 10^{-4} and 10^{-1}.

At the outset of the proton on bismuth work it was hoped that the K-capture of Po^{206} and Po^{207} could be measured by direct comparison of their Geiger activities with the Geiger activity of At^{211}. To this end samples of Po^{206} and Po^{207} were examined in the beta spectrometer of R. W. Hayward.[24] The results clearly indicated the unfeasibility of such a method. However, the results are of some interest and are therefore given in Figs. 20 and 21. It appears likely that further work in this direction could furnish valuable information on the nuclear energy levels of these isotopes and should be pursued.

Returning to a consideration of the proton induced reaction one notices that the Bi(p,γ) cross section rises to a maximum of half a millibarn at a point well above the (p,2n) threshold. Since this is unexpectedly high we might compare it with observed values of the inverse reaction (γ,p) by means of detailed balancing. The best values available are those of Hirzel and Wafflen[25] using 17.5 Mev gammas; from these (for Z from 20 to 50) one estimates the Bi(γ,p) cross section to be about 2.5 millibarns. By detailed balance using 15 Mev for the proton energy and 20 Mev for the gamma energy one gets from this

(γ,p) cross section a value of 5×10^{-6} barn for the (p,γ) reaction. This is only 1 percent of the observed value. However, due to the uncertainties of the estimated (γ,p) cross section and of the energies involved, the lack of agreement is not too disturbing. One might also compare the observed (p,γ) cross section at 15 Mev with observed values for the (n,γ) reaction since this is well above the proton potential barrier. Unfortunately here again the available data has to be extrapolated, the nearest data being for 5 Mev neutrons on gold.[26] From the gold data one estimates a $Bi(n,\gamma)$ cross section of 5 millibarns for 15 Mev neutrons; this is ten times the observed (p,γ) value. Thus one finds that the observed (p,γ) cross section is in fair agreement with other related experimental data. The question then arises as to why the statistical theory does not predict the observed cross section. The main difficulty appears to lie in the low gamma emission probability predicted by the theory. The theory has assumed that dipole transitions are greatly reduced by correlation between the motions of the nucleons. However, for the energy involved here (the kinetic energy of the proton plus its binding is approximately 20 Mev) these correlations may cease to exist.[27,28] In fact calculations of Levinger and Bethe[28] indicate that previous results based on reduced dipole transitions are too small by a factor of 10 to 100. These later calculations thus bring the theory and experiment into quite good agreement.

It would be interesting to test the theory of neutron evaporation from excited nuclei by comparing the observed and calculated values for cross sections of reactions resulting from the emission of 2 neutrons. The theoretical equation for such cross sections has been given above

and is

$$\frac{\sigma(a,2n)}{\sigma_a} = 1 - \left(1 + \frac{\Delta\varepsilon}{kT}\right) e^{-\Delta\varepsilon/kT}$$

where σ_a is the compound nucleus cross section for a bombarding particle a, and $\Delta\varepsilon$ and kT have the same meaning as before. A comparison with experiment is not as straightforward as one would like. The alpha bombardment data does not include the Bi(α,n) reaction and consequently one has no experimental value of σ_α. In the region of interest, between the (α,2n) and the (α,3n) thresholds, the fit of the theory to the experimental data is not good enough to justify substituting the calculated σ_α for the missing experimental σ_α. The deuteron data clearly indicate the simple theory as developed by Weisskopf is inadequate and consequently again one does not know what to use for the experimental compound nucleus cross section. The proton data is the only remaining hope for testing the theory and it has one serious shortcoming. The Po^{209} cross section depends on the Po^{209} half-life which is based on the theoretical yield calculations. However, if we ignore this fact and assume the true value of the half-life to be 100 years we have experimental values of σ_p and $\sigma_{p,2n}$. We can make the fit to the theory by adjusting the nuclear temperature kT and the Bi(p,2n) threshold in the following way. One constructs a graph of values of

$$f(x) \equiv 1 - \left(1 + \frac{\Delta\varepsilon}{kT}\right) e^{-\Delta\varepsilon/kT}$$

as a function of $x \equiv \Delta\varepsilon/kT$. Then one makes a table of experimental values of $\frac{\sigma_{p,2n}}{\sigma_p}$; for each of these values one enters the above graph on the f(x)-scale and finds a corresponding value on the x-scale. One then has an experimental $\Delta\varepsilon/kT$ and corresponding bombarding proton

energy. If experiment and theory agreed exactly these quantities would have a linear relationship. A plot of these is given in Fig. 22. Except for the low energy data the results fall close to a straight line. The intercept on the energy scale gives the (p,2n) threshold as 10.1 Mev and the slope gives the nuclear temperature kT as 1.17 Mev. The deviation from a straight line at low energies can be attributed in part at least to spread in the proton beam energy. The value of 1.17 Mev for the nuclear temperature kT agrees remarkably well with the value of 1.18 Mev derived from Weisskopf's calculations.[2] The (p,2n) threshold of 10.1 Mev seems reasonable since the proton binding energy is approximately 6 Mev and the neutron binding energy approximately 8 Mev. If one makes a mass-energy balance using the masses of Stern[29] a value is obtained of 7.3 Mev plus the energy of the neutrino of the Po^{208} decay; if one assumes this neutrino energy to be 2 Mev the agreement is certainly better than the uncertainties involved in the calculation.

One can also use these values of 10.1 and 1.2 together with the interpolated values of σ_p based on $r_o = 1.43 \times 10^{-13}$ cm and get calculated values for $\sigma_{p,2n}$. These results, shown as a solid curve, are compared with the experimental results in Fig. 23. Very little improvement in fit can be obtained by varying the Po^{209} half-life or the energy of the experimental data. Agreement can be secured by increasing the theoretical value of σ_p. This would also give better agreement with the experimental σ_p in this region which is based on a Po^{209} half-life of 100 years.

The author wishes to thank Prof. E. Segrè for his continued guid-

ance and invaluable discussions throughout this work. The author is indebted to Prof. E. O. Lawrence for permission to use the facilities of the Radiation Laboratory and for his stimulating interest in the problem. Thanks are due to Dr. R. L. Leininger for the many chemical separations and for the preparation of the thin samples, to Mr. A. Ghiorso for the alpha pulse analysis, and to Dr. R. Hayward for permission to use his electron spectrometer. The splendid cooperation of the operating crews of the several accelerators used is also gratefully acknowledged.

This work was performed under the auspices of the Atomic Energy Commission.

References

1. N. Bohr, Nature 137, 344 (1936).

2. AEC Declassified Document MDDC-1175 (1947), Lecture Series in Nulcear Physics, LA24, Chapter 36, p. 105.

3. D. C. Peaslee, Phys. Rev. 74, 1001 (1948).

4. D. G. Hurst, R. Lantham, and W. B. Lewis, Proc. Roy. Soc. 174, 126 (1940).

5. J. M. Cork, J. Halpern, and H. Tatel, Phys. Rev. 57, 348 (1940); 57, 371 (1940).

6. R. S. Krishnan and E. Z. Nahum, Proc. Roy. Soc. A180, 321 (1942).

7. J. M. Cork, Phys. Rev. 70, 563 (1946).

8. D. R. Corson, K. R. MacKenzie, and E. Segrè, Phys. Rev. 58, 672 (1940).

9. For the separation methods see Johnson, Leininger, and Segrè, "Chemical properties of astatine. I," J. Chem. Phys. 17, 1 (1949).

10. A. W. Vance, Rev. Sci. Inst. 7, 489 (1936).

11. R. R. Wilson, Phys. Rev. 60, 749 (1941).

12. M. Stanley Livingston and H. A. Bethe, Rev. Mod. Phys. 9, 285 (1937).

13. J. H. Smith, Phys. Rev. 71, 32 (1947).

14. E. L. Kelly, Phys. Rev. 75, 1006 (1949).

15. D. H. Templeton, J. J. Howland, and I. Perlman, Phys. Rev. 72, 758, (1947).

16. D. H. Templeton, Phys. Rev. 78, 312 (1950).

17. Ghiorso, Jaffey, Robinson, and Weissbourd, "An alpha-pulse analyser apparatus," Plutonium Project Record 14B, 17.3 (1948).

18. D. G. Karraker and D. H. Templeton, unpublished data.

19. W. M. Brobeck, E. O. Lawrence, et al., Phys. Rev. 71, 449 (1947).

20. L. R. Henrich, D. C. Sewell, and J. Vale, Rev. Sci. Inst. 20, 887 (1949).

21. W. M. Powell, et al., Rev. Sci. Inst. 19, 506 (1948).

22. L. W. Alvarez, et al., UCRL Report 236.

23. Weisbluth, Putnam, and Segrè, private communication.

24. R. W. Hayward, UCRL Report 582 (Ph.D. Thesis).

25. O. Hirzel and H. Wäfflen, Helv. Phys. Acta 20, 373 (1947) and 21, 200 (1948).

26. R. K. Adair, Rev. Mod. Phys. 22, 249 (1950).

27. M. Goldhaber and E. Teller, Phys. Rev. 74, 1046 (1948).

28. J. S. Levinger and H. A. Bethe, Phys. Rev. 78, 115 (1950).

29. M. O. Stern, Rev. Mod. Phys. 21, 316 (1949).

Table I.

Experimental values of the cross section for the $Bi(\alpha,2n)At^{211}$ and the $Bi(\alpha,3n)At^{210}$ reactions at various energies of the bombarding alpha-particles.

α-energy Mev	σAt^{211} Run I barns	σAt^{211} Run II barns	σAt^{211} Run III barns	σAt^{210} Run I barns	σAt^{210} Run II barns	σAt^{210} Run III barns
18.8		0.000				
19.9	0.000					
20.0			0.000			
20.2		0.001				
21.2	0.01					
21.6		0.01	0.03			
22.4	0.10					
23.0		0.11				
23.1			0.16			
23.5	0.25					
24.2		0.29				
24.6	0.40		0.35			
25.4		0.45				
25.7	0.55					
26.1			0.57			
26.5		0.58				
26.7	0.67					
27.4			0.71			0.000
27.6		0.69			0.000	
27.7	0.75			0.000		
28.6	0.83		0.81	0.004		0.004
28.7		0.78			0.003	
29.6	0.90			0.013		
29.7		0.85			0.007	
29.9			0.90			0.015
30.5	0.89			0.06		
30.7		0.89			0.05	
31.0			0.91			0.10
31.4	0.86			0.17		
31.7		0.85			0.16	
32.2			0.81			0.28
32.3	0.75			0.35		
32.6		0.75			0.37	
33.1	0.62			0.53		
33.3			0.63			0.53
33.6		0.61			0.61	
34.0	0.48			0.73		
34.5			0.46			0.75
34.6		0.47			0.82	
34.8	0.39			0.93		
35.5		0.37			1.01	
35.6	0.30		0.33	1.03		0.94
36.4	0.24	0.29		1.14	1.16	
36.7			0.25			1.11
37.2	0.20	0.23		1.20	1.21	
38.0	0.17			1.24		
38.8	0.15			1.27		

Table II.

Experimental values of the cross section for the Bi(d,p)RaE, the Bi(d,n)Po^{210}, the Bi(d,2n)Po^{209}, and the Bi(d,3n)Po^{208} reactions at various energies of the bombarding deuterons.

	σRaE		σPo^{210}		σPo^{209}			σPo^{208}	
d-energy Mev	Run I barns	Run II barns	Run I barns	Run II barns	Run I barns	Run I* barns	Run II barns	Run I barns	Run II barns
5.3		0.0002							
5.9		0.001							
6.0	0.001								
6.5	0.002	0.002	0.0003	0.0003					
7.0	0.004		0.0006						
7.1		0.005		0.001					
7.5	0.008		0.001		0				
7.6		0.009		0.002			0		
7.9	0.014		0.002		0.005				
8.1		0.016		0.004			0.007		
8.3	0.021		0.004		0.015				
8.6		0.026		0.007			0.007		
8.7	0.030		0.006			0.013			
9.0	0.040	0.037	0.009	0.010	0.028		0.022		
9.4	0.051	0.051	0.011	0.013	0.05		0.05		
9.7	0.062		0.014		0.05				
9.8		0.064		0.017			0.06		
10.1	0.073		0.016		0.10	0.09			
10.2		0.076		0.020			0.10		
10.4	0.082		0.019		0.09				
10.6		0.084		0.023			0.12		
10.7	0.091		0.023		0.16				
11.0	0.099	0.095	0.026	0.026	0.17		0.18		
11.3	0.104		0.028		0.19	0.21			
11.4		0.100		0.028			0.25		
11.6	0.108		0.029		0.26				
11.8		0.105		0.029			0.23		
11.9	0.111		0.030		0.28				
12.2	0.112	0.107	0.030	0.031	0.30		0.30		
12.5	0.114	0.109	0.030	0.031			0.34		
12.8	0.114		0.031		0.39				
12.9		0.108		0.029					
13.1	0.113		0.030						
13.2		0.108		0.031			0.41		0
13.3	0.113		0.030			0.42			
13.5	0.112	0.107	0.031	0.031	0.54			0	0.004
13.7	0.110		0.033					0.003	
13.8		0.102		0.031					0.010
14.0	0.109		0.032					0.008	
14.1		0.102		0.030			0.44		0.012
14.3	0.106		0.030		0.53			0.023	
14.5	0.104	0.098	0.031	0.030				0.028	0.03
14.8	0.101	0.095	0.031	0.031				0.04	0.04

d-energy Mev	σRaE Run I barns	σRaE Run II barns	σPo^{210} Run I barns	σPo^{210} Run II barns	σPo^{209} Run I barns	σPo^{209} Run I* barns	σPo^{209} Run II barns	σPo^{208} Run I barns	σPo^{208} Run II barns
15.1	0.096	0.093	0.032	0.031	0.56		0.49	0.07	0.08
15.3	0.097		0.030					0.10	
15.4		0.088		0.030					0.12
15.55	0.094		0.032					0.12	
15.7		0.086		0.031					0.14
15.8	0.091		0.030		0.47	0.56		0.17	
16.0		0.082		0.029			0.57		0.20
16.05	0.089		0.030					0.21	
16.3	0.084	0.081	0.030	0.030				0.25	0.24
16.5	0.084		0.031		0.54			0.29	
16.6		0.078		0.030					0.32
16.75	0.084		0.031					0.32	
16.9		0.077		0.030			0.39		0.36
17.0	0.082		0.031					0.38	
17.1		0.073		0.032					0.40
17.2	0.079		0.031		0.41			0.43	
17.4	0.074	0.071	0.031	0.031		0.38		0.47	0.48
17.7	0.075	0.070	0.030	0.032				0.52	0.51
17.9	0.074		0.032					0.56	
18.0		0.067		0.032		0.37			0.57
18.1	0.072		0.030					0.61	
18.3	0.073	0.067	0.032	0.029	0.37			0.64	0.62
18.5	0.070	0.066	0.032	0.031		0.28		0.68	0.65
18.7	0.068		0.030					0.71	

Table III.

Experimental values for the At^{211} yield in a bismuth and aluminum foil stack bombarded by the 184-inch cyclotron electrostatically deflected alpha-beam for various absorber thicknesses in the foil stack. Corresponding mean beam energies are also given.

Al Absorber mg cm^{-2}	Mean Range mg cm^{-2} Al	Mean Energy Mev	σ barns
0.016	9.384	388	1.22×10^{-4}
1.143	8.257	360	1.85
2.264	7.136	332	1.99
3.382	6.018	300	2.03
4.409	4.991	272	2.44
5.271	4.129	245	3.30
5.959	3.441	220	4.27
6.648	2.752	194	5.42
7.340	2.060	166	8.36
7.884	1.516	138	1.32×10^{-3}
8.281	1.119	117	2.14
8.463	0.937	106	2.79
8.574	0.826	99	3.57
8.649	0.751	94	4.53
8.760	0.640	86	6.35
8.834	0.566	81	8.36
8.906	0.494	75	1.19×10^{-2}
8.933	0.467	72	1.38
8.969	0.431	69	1.80×10^{-2}
9.004	0.396	66	2.60
9.041	0.359	62	3.41
9.078	0.322	58	5.04
9.114	0.286	54	7.23
9.151	0.249	50	9.16
9.186	0.214	46	1.17×10^{-1}
9.222	0.178	41	1.31
9.258	0.142	36.5	1.50
9.294	0.106	31	1.55
9.329	0.071	24.5	1.44
9.363	0.037	16.5	1.31
9.399	0.001	0	1.01
9.436			6.70×10^{-2}
9.472			3.65
9.508			1.60
9.543			6.0×10^{-3}

Table IV.

Experimental values of the cross section for the $Bi(p,\gamma)Po^{210}$, the $Bi(p,n)Po^{209}$, the $Bi(p,2n)Po^{208}$, the $Bi(p,3n)Po^{207}$, and the $Bi(p,4n)Po^{206}$ reactions at various energies of the bombarding protons.

p-energy Mev	Range in Bi mg/cm^2	σPo^{210} III barns	σPo^{209} III barns	σPo^{208} I barns	σPo^{208} II barns	σPo^{208} III barns	σPo^{207} I barns	σPo^{207} II barns	σPo^{206} I barns	σPo^{206} II barns	σ for all activity treated as Po^{208} I barns	σ for all activity treated as Po^{208} II barns	σ for all activity treated as Po^{208} III barns
6.1	154	0.008×10^{-3}	0.003										0.0002
6.1_5												0.0000	
6.5	172												0.0003
6.9	190	0.028×10^{-3}	0.010										0.0005
7.0												0.0001_4	
7.3	207												0.0004
7.7	225	0.044×10^{-3}	0.020										0.0009
7.8												0.0010	
8.1	242												0.0011
8.2				0									
8.5	261	0.054×10^{-3}	0.041		0.0001	0.00026						0.0019	0.0018
8.8_5					0.0004							0.0036	
8.9	280												0.0022
9.2					0.001							0.0036	
9.2_5	300	0.099×10^{-3}	0.054			0.0016							0.0038
9.3				0.001									
9.5_5					0.002							0.005_0	
9.6_5	320												0.0068
9.8_5					0.004							0.008_6	
10.0	340	0.15×10^{-3}	0.086			0.0069							0.0106
10.1_5					0.009							0.015	
10.35	360												0.019
10.5					0.017							0.023	
10.6				0.015									
10.7	380	0.25×10^{-3}	0.119			0.025							0.030
10.8					0.029							0.037	
11.0_5	400												0.049
11.1					0.048							0.05_8	
11.3_5	420	0.29×10^{-3}	0.162			0.067							0.074
11.4					0.07_1							0.08_2	

p-energy Mev	Range in Bi mg/cm²	σPo²¹⁰ III barns	σPo²⁰⁹ III barns	I barns	σPo²⁰⁸ II barns	III barns	σPo²⁰⁷ I barns	II barns	σPo²⁰⁶ I barns	II barns	σ for all activity treated as Po²⁰⁸ I barns	II barns	III barns
11.7	440				0.11							0.12	0.11
11.75				0.115									
11.95					0.14							0.15	
12.0	461	0.45 x10⁻³	0.160			0.138							0.15
12.3	481												0.20
12.45					0.23								
12.65	502	0.45 x10⁻³	0.162			0.24							0.24
12.85				0.30									
12.9					0.32								
13.0	523												0.30
13.3	544	0.52 x10⁻³	0.114			0.35							0.35
13.4					0.41								
13.6	565												0.41
13.8					0.50								
13.9	587	0.46 x10⁻³	0.107			0.47							
14.0				0.54									
14.25	609				0.58	0.53							
14.55	631	0.54 x10⁻³	0.072			0.58							
14.65					0.64								
14.85	653					0.63							
15.05					0.71								
15.1				0.74									
15.15	675	0.66 x10⁻³	0.041			0.68							
15.45	697					0.72							
15.55					0.76								
15.75	720	0.90 x10⁻³	0.045			0.75							
16.05	743				0.83	0.80							
16.2				0.88									
16.35	766					0.83							
16.5					0.88								
16.65	789					0.86							
16.95	813					0.89							
17.0					0.90								
17.2				0.97									

p-energy Mev	Range in Bi mg/cm^2	σPo^{210} III barns	σPo^{209} III barns	σPo^{208} I barns	II barns	III barns	σPo^{207} I barns	II barns	σPo^{206} I barns	II barns	σ for all activity treated as Po^{208} I barns	II barns	III barns
17.25	837					0.92							
17.4					0.93								
17.55	861	0.62 x10^{-3}				0.95							
17.85	885					0.98							
17.9					0.99								
18.15	910					1.00							
18.3				1.07									
18.4					1.01								
18.45	935					1.02							
18.75	959					1.05							
18.9					1.05			0					
19.05	985					1.07							
19.35	1010					1.07							
19.4				1.12	1.07			0.05					
19.7	1037					1.07							
19.8					1.07			0					
20.0	1065	0.30 x10^{-3}				1.06							
20.3	1092				1.04	1.04		0.12					
20.4				1.17			0.15						
20.6	1121					1.01							
20.7					1.02			0.13					
20.9	1149					0.97							
21.2	1177				0.96	0.94		0.18					
21.5				0.96			0.34						
21.55	1206					0.88							
21.6					0.89			0.44					
21.85	1235					0.82							
22.0					0.79			0.46					
22.15	1265					0.75							
22.45	1295					0.70							
22.5					0.70			0.67					
22.55				0.73			0.68						
22.75	1325					0.63							
23.0					0.59			0.95					

p-energy Mev	Range in Bi mg/cm^2	σPo^{210} III barns	σPo^{209} III barns	σPo^{208} I barns	σPo^{208} II barns	σPo^{208} III barns	σPo^{207} I barns	σPo^{207} II barns	σPo^{206} I barns	σPo^{206} II barns	σ for all activity treated as Po^{208} I barns	σ for all activity treated as Po^{208} II barns	σ for all activity treated as Po^{208} III barns
23.1	1356					0.57							
23.4	1387					0.52							
23.5					0.52			1.03					
23.6				0.52			1.11						
23.7	1418	0.16 x10^{-3}	0.017			0.47							
23.95					0.44			0.91					
24.0	1449					0.42							
24.3	1481					0.38							
24.4					0.38			1.25					
24.6	1513					0.35							
24.7				0.36			1.29						
24.9					0.32$_5$			1.14					
24.95	1545					0.31$_5$							
25.25	1577					0.29$_2$							
25.3					0.28$_5$			1.22					
25.55	1609					0.27$_0$							
25.8				0.26	0.25$_5$		1.38	1.31					
25.85	1641					0.24$_4$							
26.15	1673					0.22$_6$							
26.2					0.23$_5$			1.28					
26.45	1706					0.21$_0$							
26.75	1739	0.19 x10^{-3}	0.045		0.20	0.20$_2$		1.27					
26.8				0.21			1.41						
27.05	1771					0.19$_4$							
27.2					0.19			1.40					
27.65	1837					0.17$_4$							
27.7					0.18			1.55		0			
27.8				0.17			1.56		0.001$_5$				
27.95	1871	0.10 x10^{-3}	0.024										
28.1					0.16$_5$			1.49		0.01$_3$			
28.3	1916					0.15$_8$							
28.6					0.16$_5$			1.40		0.02$_0$			
28.9				0.14$_5$			1.58		0.03$_8$				

p-energy Mev	Range in Bi mg/cm^2	σPo^{210} III barns	σPo^{209} III barns	σPo^{208} I barns	σPo^{208} II barns	σPo^{208} III barns	σPo^{207} I barns	σPo^{207} II barns	σPo^{206} I barns	σPo^{206} II barns	σ for all activities treated as Po^{208} I barns	σ for all activities treated as Po^{208} II barns	σ for all activities treated as Po^{208} III barns
29.0					0.145			1.47		0.048			
29.1	2007					0.146							
29.5					0.145			1.45		0.083			
29.9	2098			0.13	0.14	0.133	1.52	1.45	0.135	0.13			
30.4					0.125			1.55		0.21			
30.65	2191					0.128							
30.8					0.13			1.36		0.27			
30.9				0.12			1.38		0.31				
31.05	2237	0.07 x10^{-3}	0.021										
31.3					0.13			1.19		0.38			
31.9				0.14			1.31		0.525				

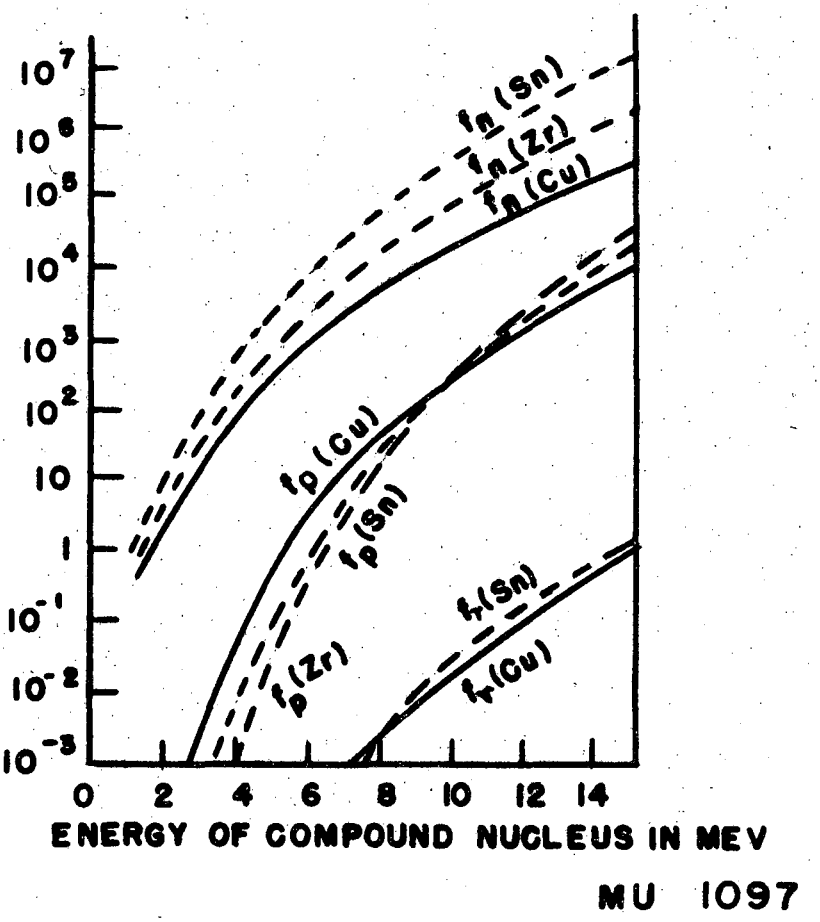

Fig. 1. The relative emission probability functions f_n, f_p, and f_γ are given as functions of the excitation energy above the ground state of the residual nucleus. These values must be multiplied by 2 or 0.5 if the residual nucleus is odd-odd or even-even, respectively.

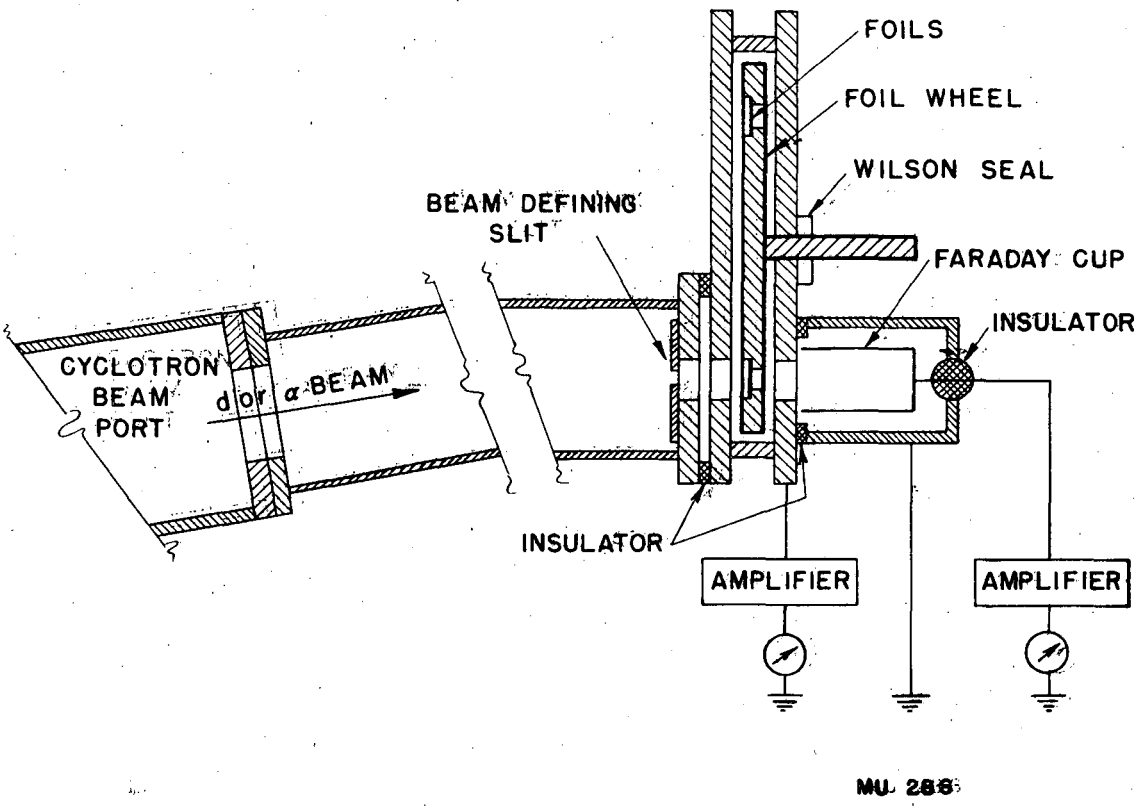

Fig. 2. Schematic diagram of the collimating tube, foil holder, and current amplifiers. This apparatus connects directly to the cyclotron tank and becomes therefore an integral part of the cyclotron vacuum system, obviating the need for any windows or separate pumps.

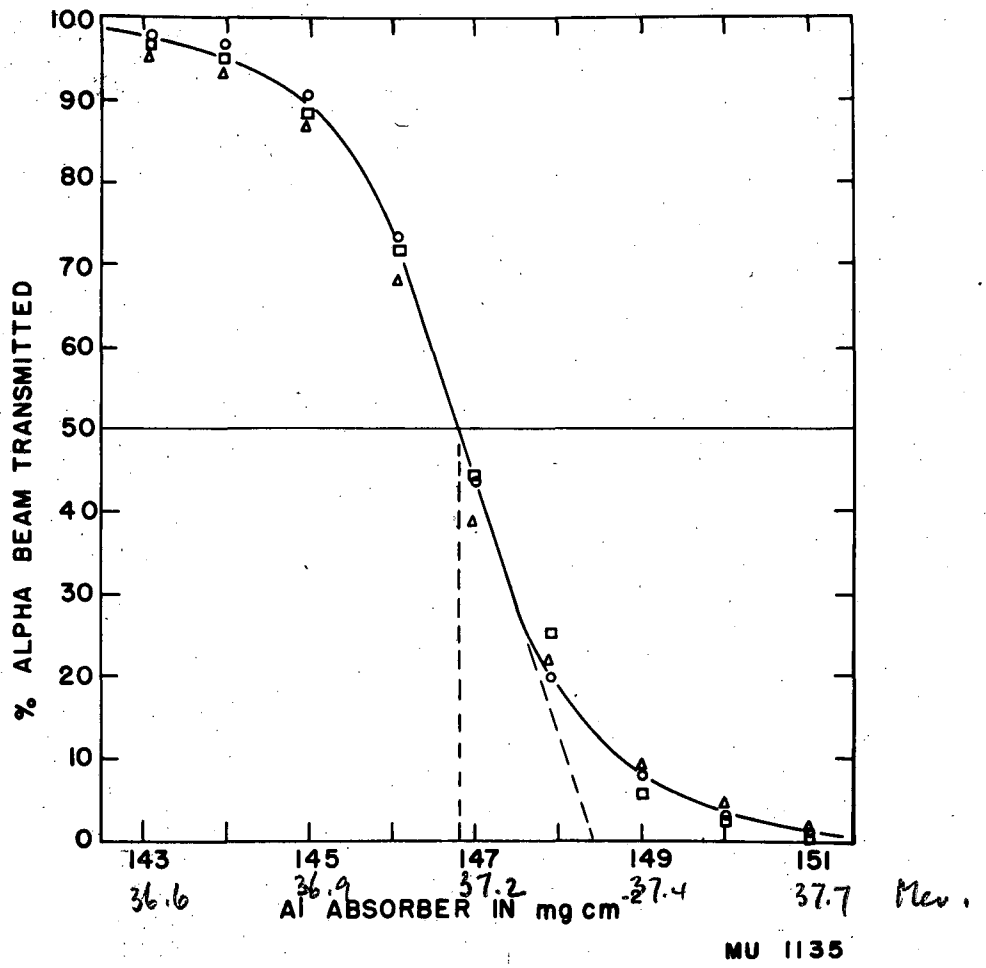

Fig. 3. The percent of the α-beam transmitted by the Al absorber plotted as a function of the absorber thickness. The three sets of points represent data taken before bombardment, at the middle of bombardment, and after bombardment of the bismuth foils. The straggling, given by the difference between the extrapolated range and the mean range divided by the mean range, is 1.1 percent.

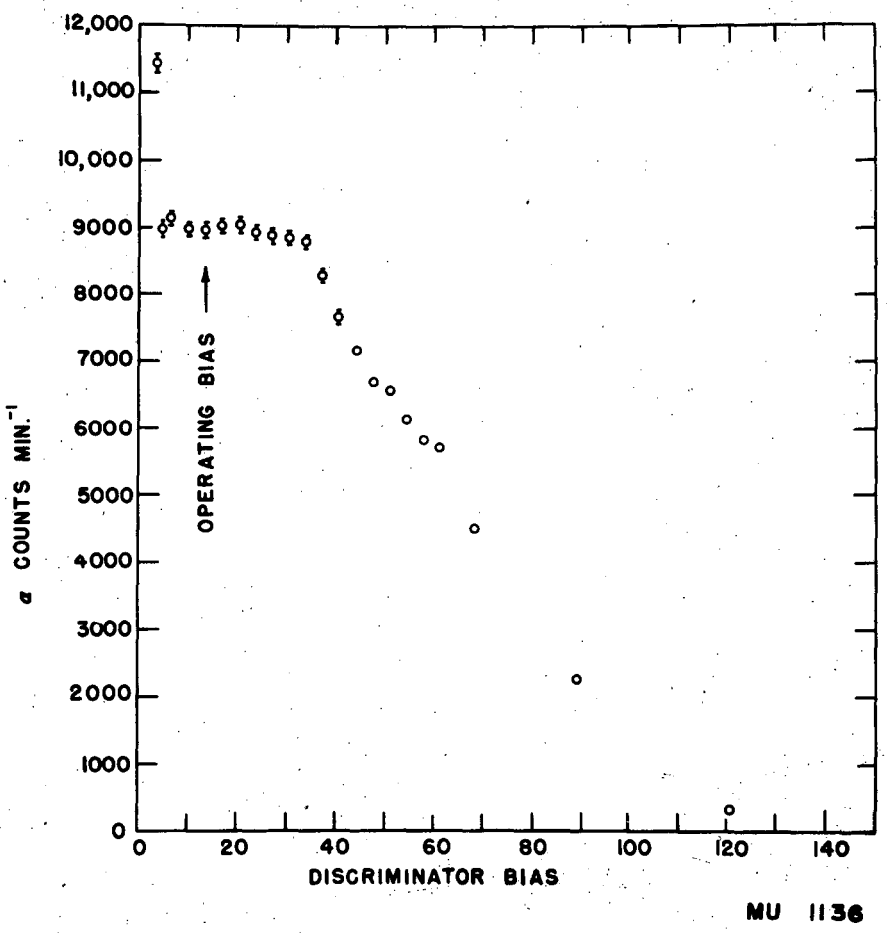

Fig. 4. Counts per minute of the thin uranium α-standard plotted as a function of the pulse discriminator bias voltage. The operating bias was kept constant to within 2 units.

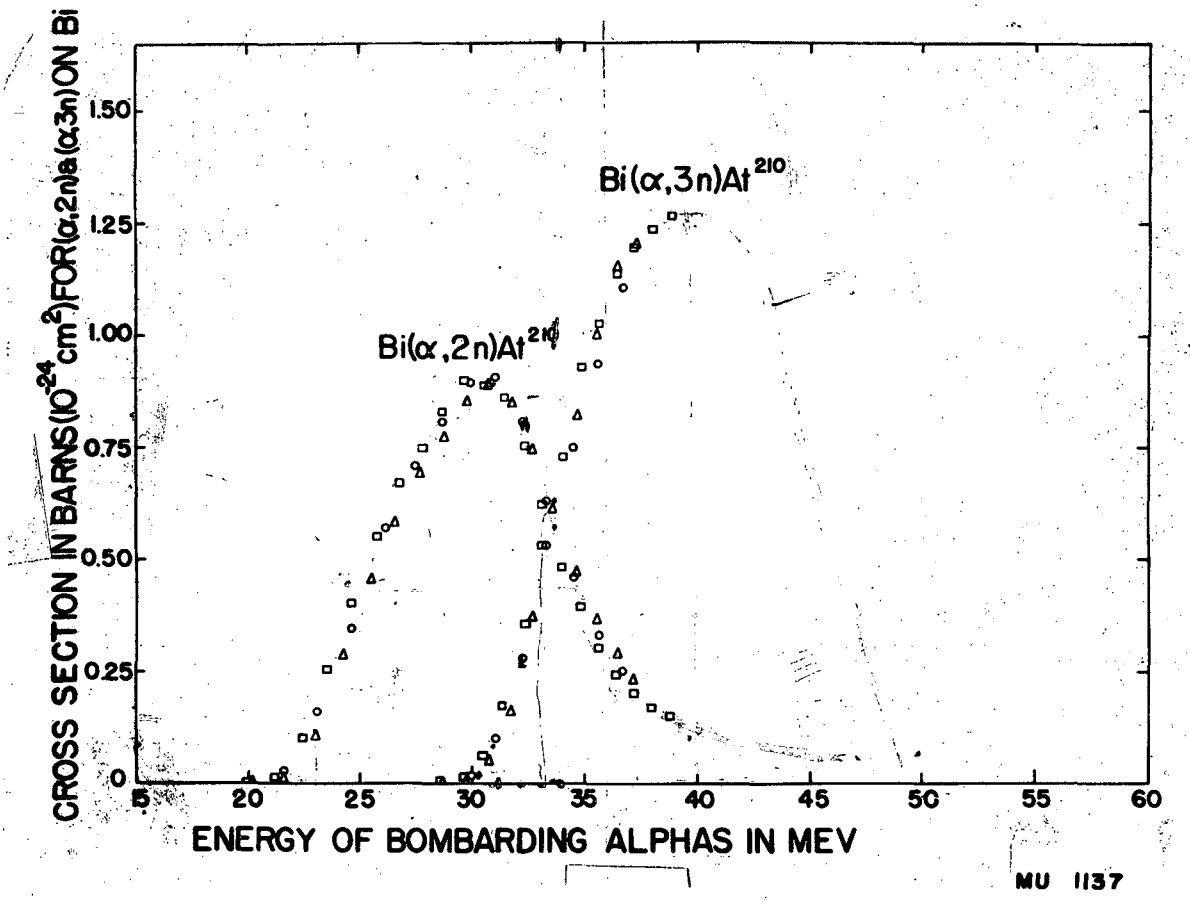

Fig. 5. Absolute cross section for the Bi(α,2n) reaction and the Bi(α,3n) reaction plotted as a function of the energy of the bombarding alphas.

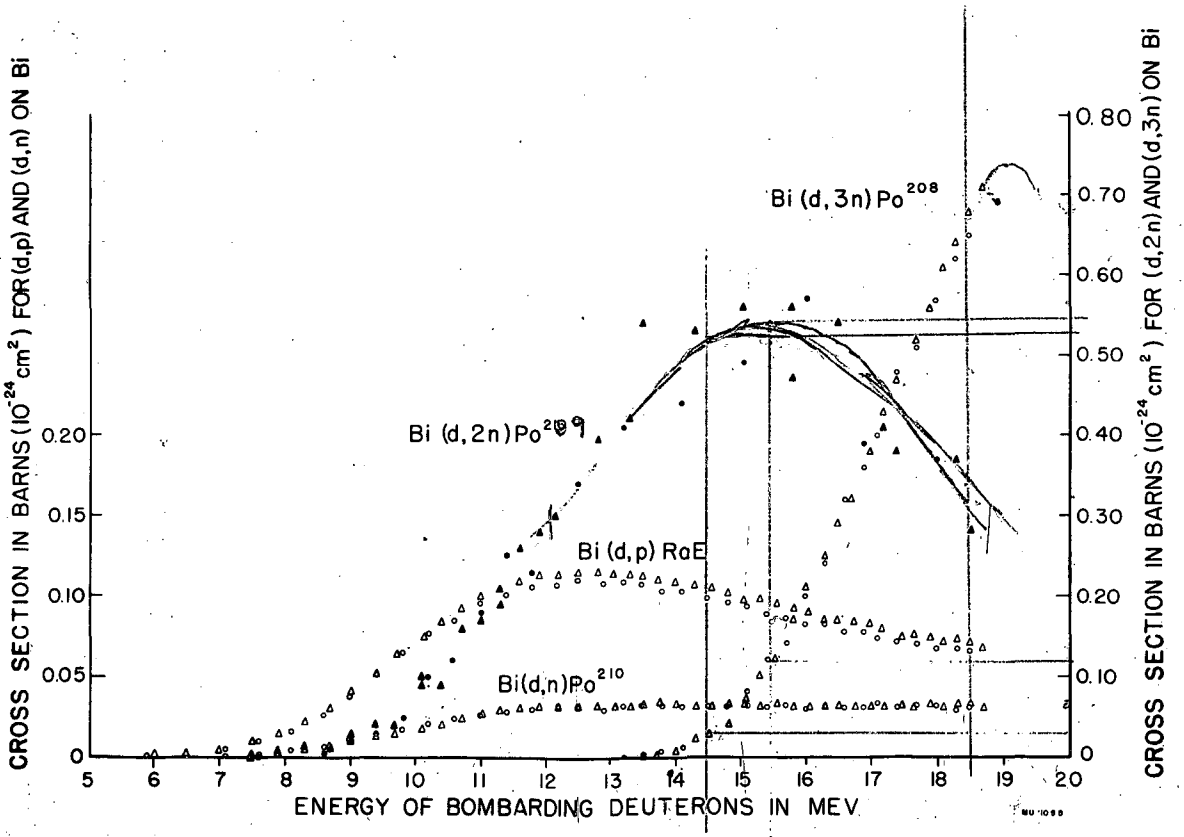

Fig. 6. Absolute cross sections for the Bi(d,p), the Bi(d,n), the Bi(d,2n), and the Bi(d,3n) reactions plotted as a function of the energy of the bombarding deuterons.

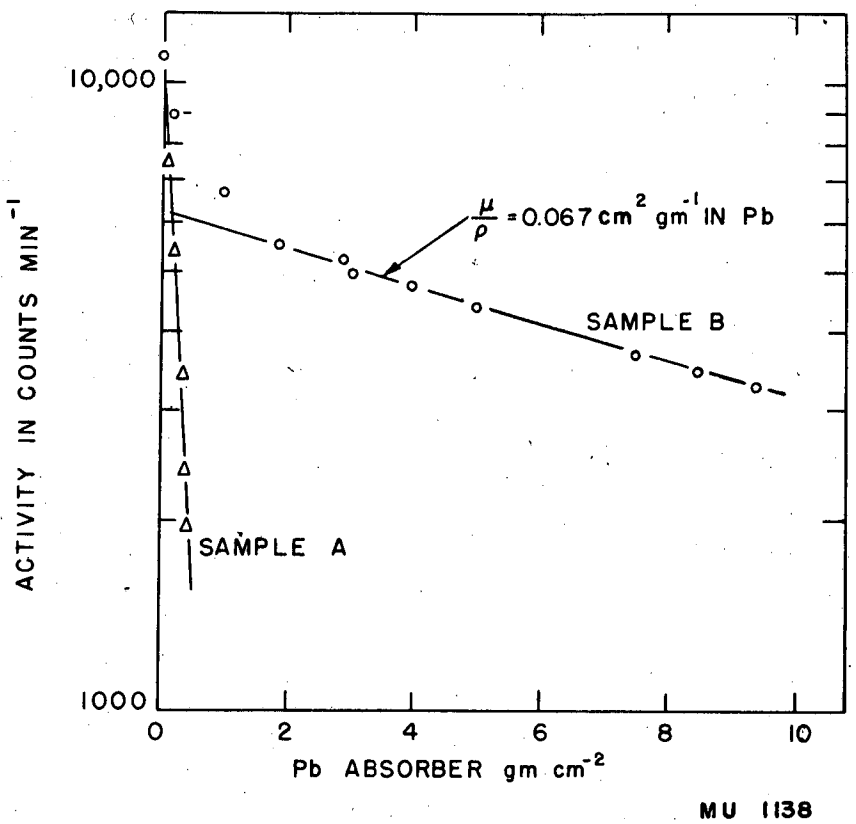

Fig. 7. The counting rate on a G-M counter of astatine samples plotted as a function of the thickness of lead absorber. Sample A consisted of the At extracted from a foil of Bi bombarded with alphas of 25 Mev energy; sample B consisted of the At extracted from a foil of Bi bombarded with alphas of 37 Mev. As a check of the geometry the mass absorption coefficient of a Co^{60} γ-standard was measured and found to be 0.055 cm^2 gm^{-1} in Pb.

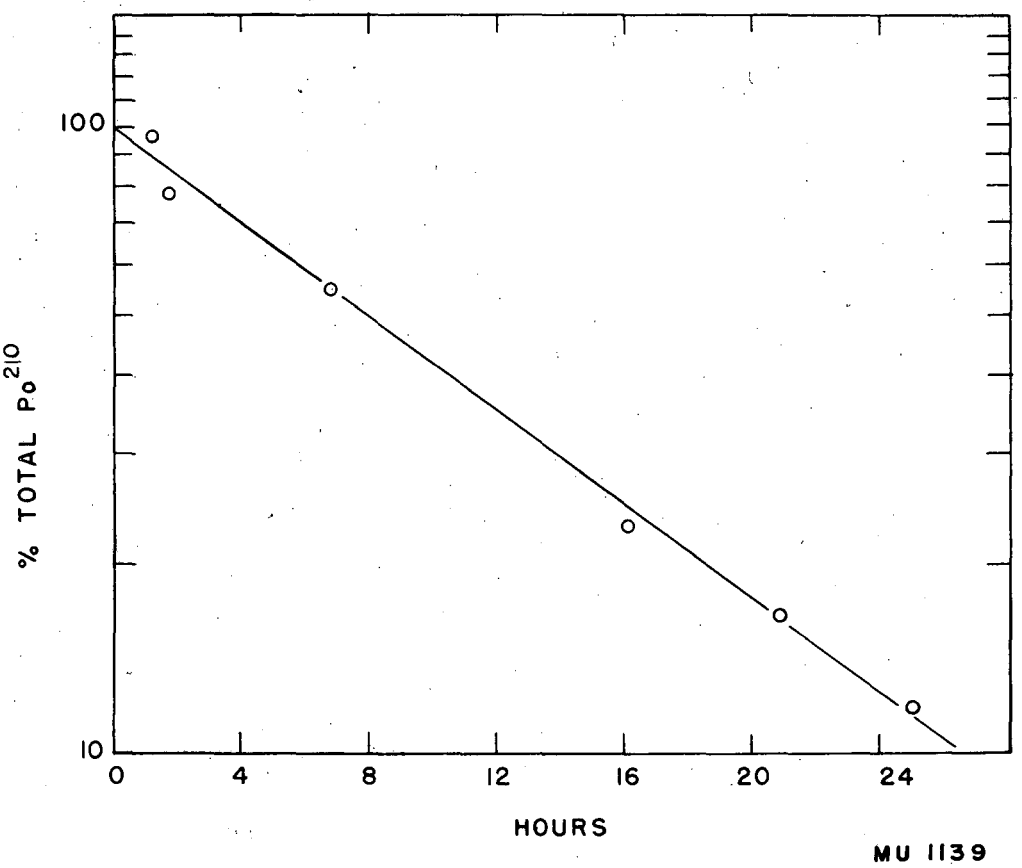

Fig. 8. The amount of Po^{210} formed by the decay of the extracted At^{210}, expressed as percent of the <u>total</u> Po^{210} formed, plotted as a function of the time from the middle of bombardment until the At extraction.

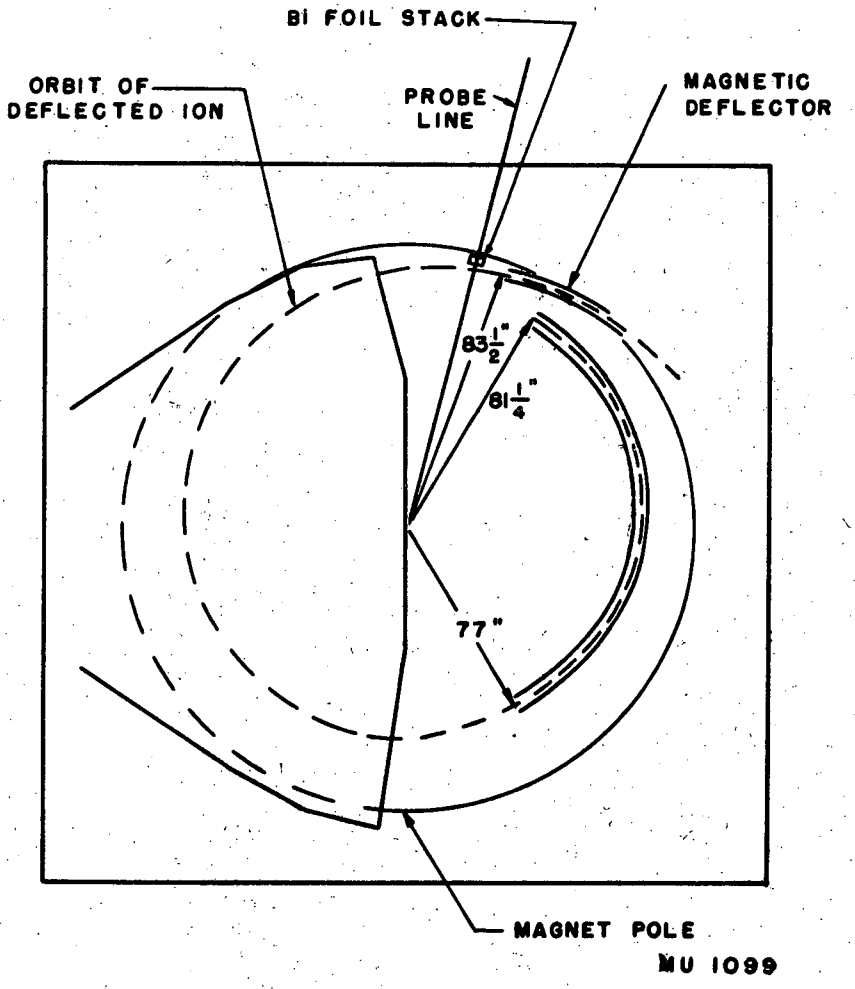

Fig. 9. Schematic diagram of the 184-inch cyclotron and the deflected beam path showing the location of the foil stack during bombardment.

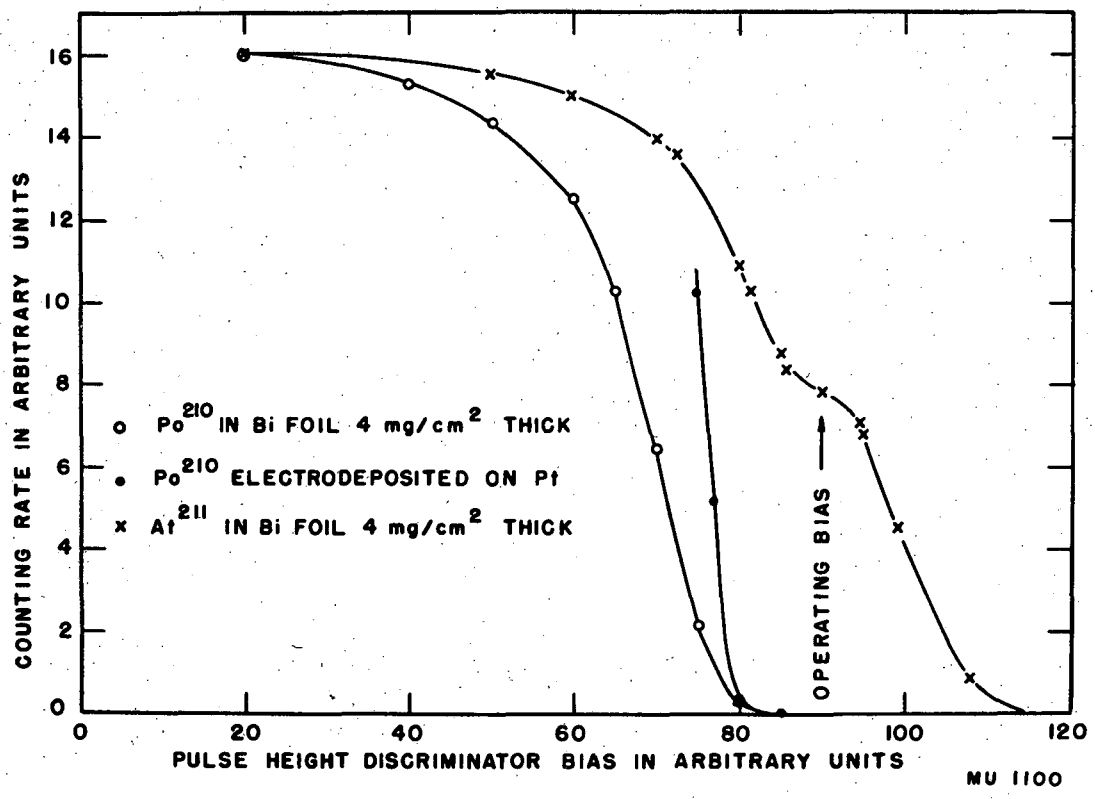

Fig. 10. Counting rate versus pulse height discriminator bias, both in arbitrary units, for "thick" and "thin" Po^{210} samples and a "thick" At^{211} sample. The separation of the alpha ranges of the At^{211} is clearly discernable even though the At^{211} is dispersed throughout a 4 mg cm^{-2} bismuth foil.

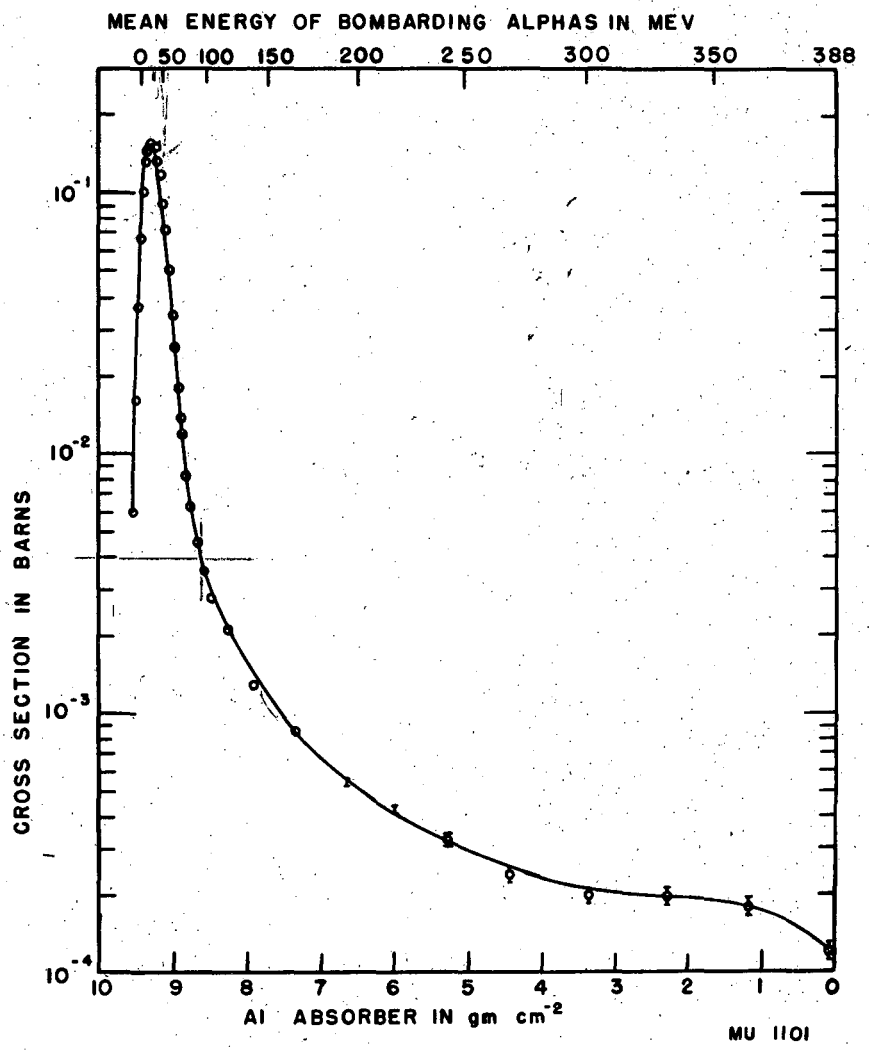

Fig. 11. Cross section for the yield of At^{211} produced in a bismuth and aluminum foil stack by alpha bombardment as a function of the aluminum absorber thickness in the primary alpha-beam; a scale of the corresponding mean beam energy is also given. The error shown is the standard deviation due to counting statistics only.

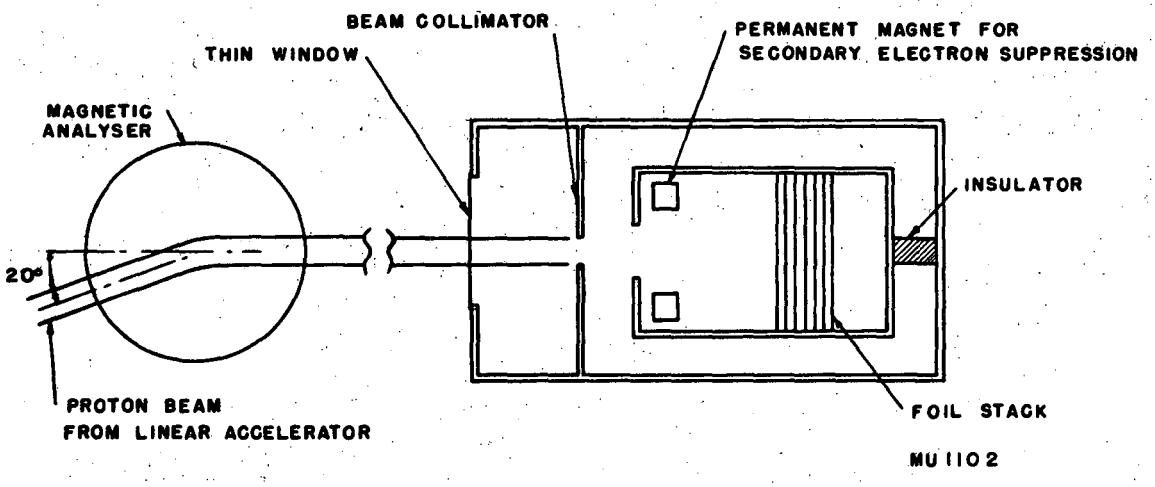

Fig. 12. Schematic diagram of the steering magnet, foil stack, and Faraday cup. The entire chamber is maintained at a high vacuum of 0.1 micron of mercury or better.

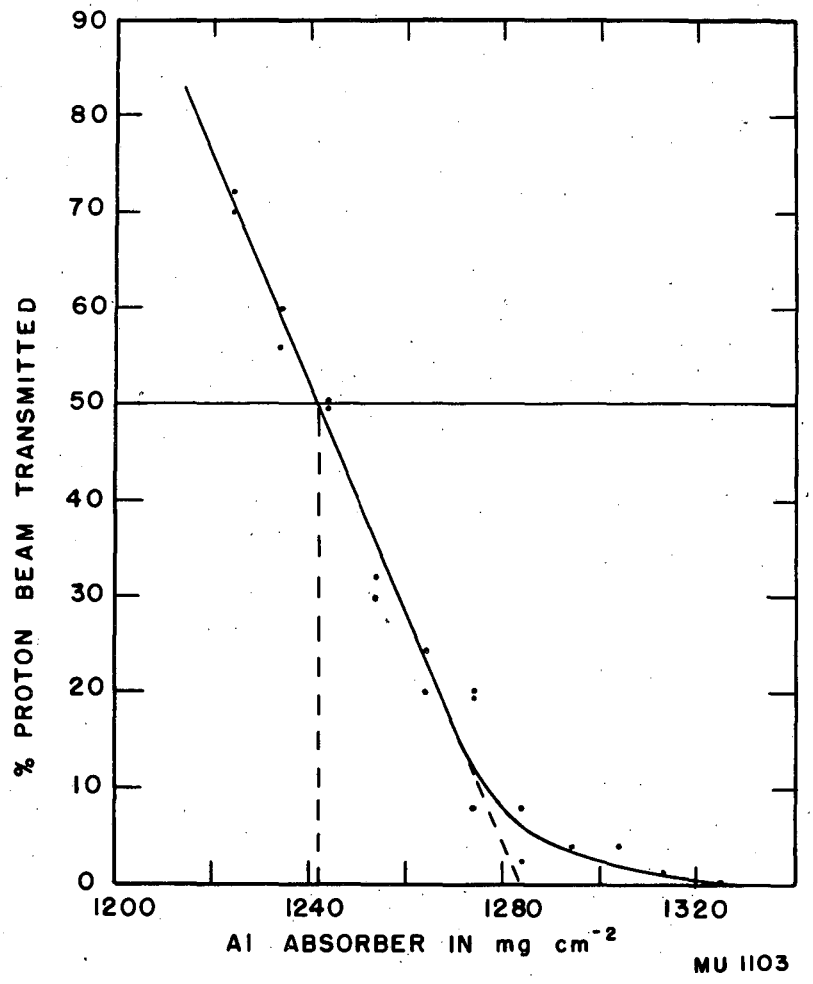

Fig. 13. The percent of the proton beam transmitted through the aluminum absorber plotted as a function of the absorber thickness. The straggling, given by the difference between the extrapolated range and the mean range divided by the mean range, is 3.2 percent..

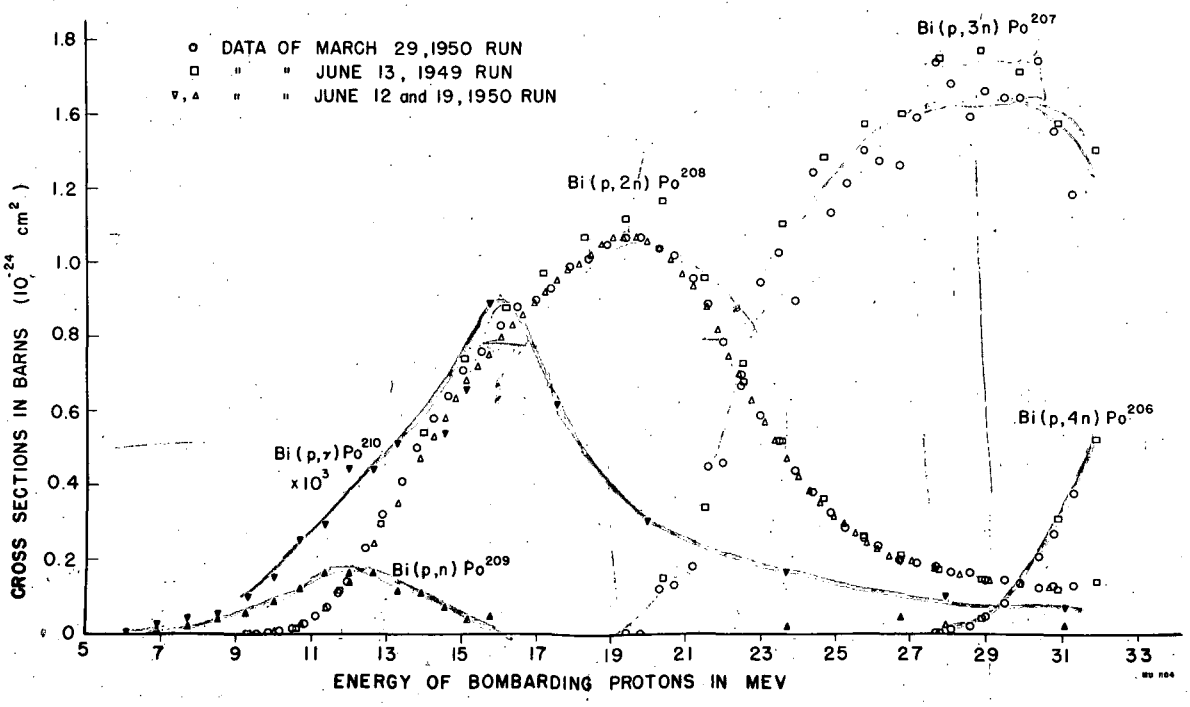

Fig. 14. Absolute cross section plotted as a function of the bombarding protons for the Bi(p,γ), the Bi(p,n), the Bi(p,2n), the Bi(p,3n), and the Bi(p,4n) reactions. The cross section for the Bi(p,γ) reaction has been plotted on a scale 10^3 times larger than the scale for the other reactions; its maximum value is somewhat less than 1 millibarn.

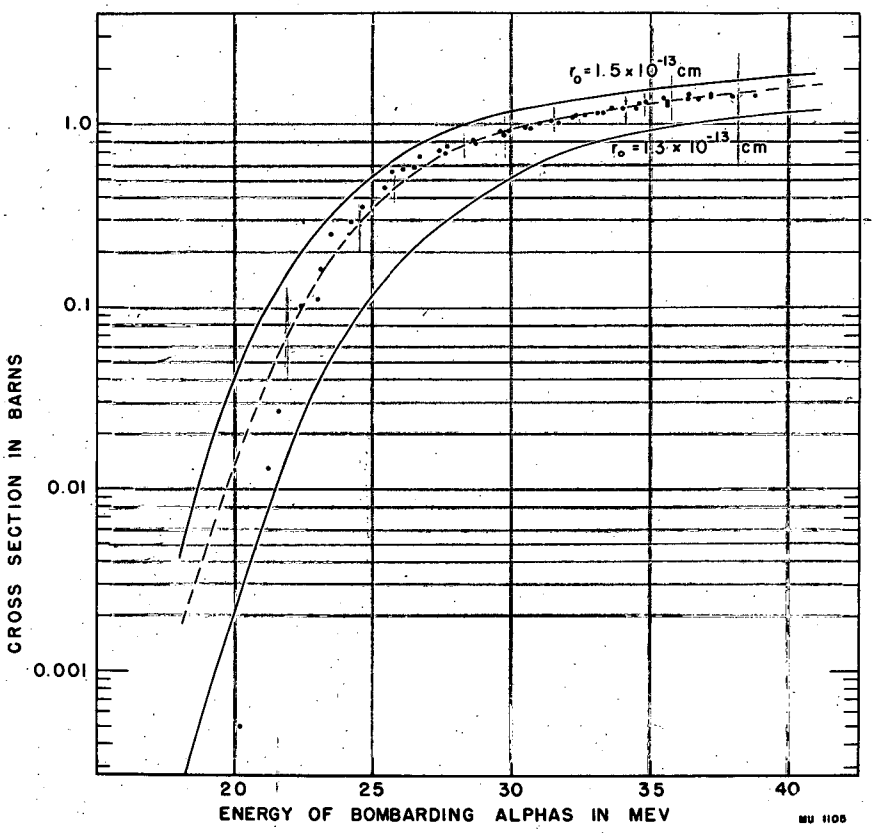

Fig. 15. Cross section plotted as a function of the energy of the bombarding alphas. Theoretical values for the Bi + α compound nucleus cross section are given by the solid and dashed curves. The points represent the sum of the experimental cross section values for the Bi(α,2n) and the Bi(α,3n) reactions.

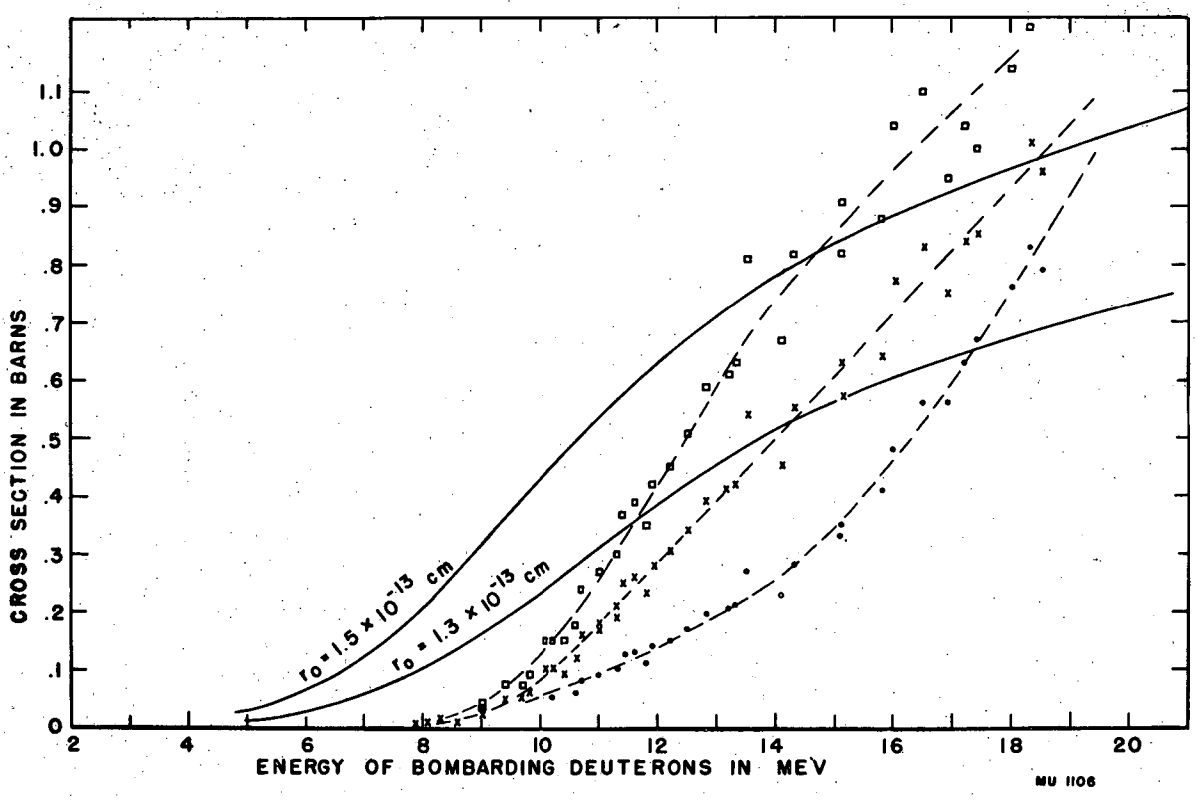

Fig. 16. Cross section plotted as a function of the energy of the bombarding deuterons. Theoretical values for the Bi + d compound nucleus cross section are given by the solid curves. The points represent the sum of the experimental cross section values for the $Bi(d,2n)Po^{209}$ and the $Bi(d,3n)Po^{208}$ reactions. The squares are based on a Po^{209} half-life of 150 years, the crosses on a Po^{209} half-life of 100 years, and the circles on a Po^{209} half-life of 50 years.

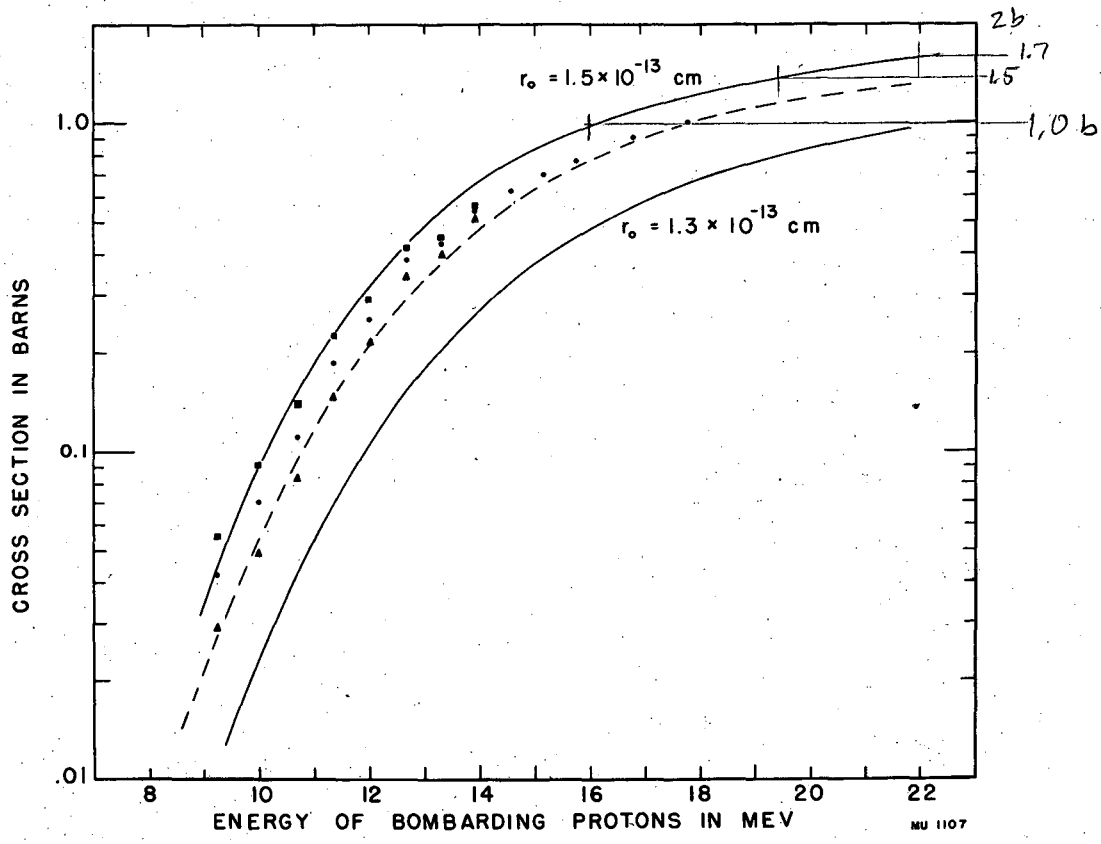

Fig. 17. Cross section plotted as a function of the energy of the bombarding protons. Theoretical values for the Bi + p compound nucleus cross section are shown by the solid and dashed curves. The points represent the sum of the experimental cross section values for the $Bi(p,n)Po^{209}$ and the $Bi(p,2n)Po^{208}$ reactions. The squares are based on a Po^{209} half-life of 100 years, the circles on a Po^{209} half-life of 75 years, and the triangles on a Po^{209} half-life of 50 years.

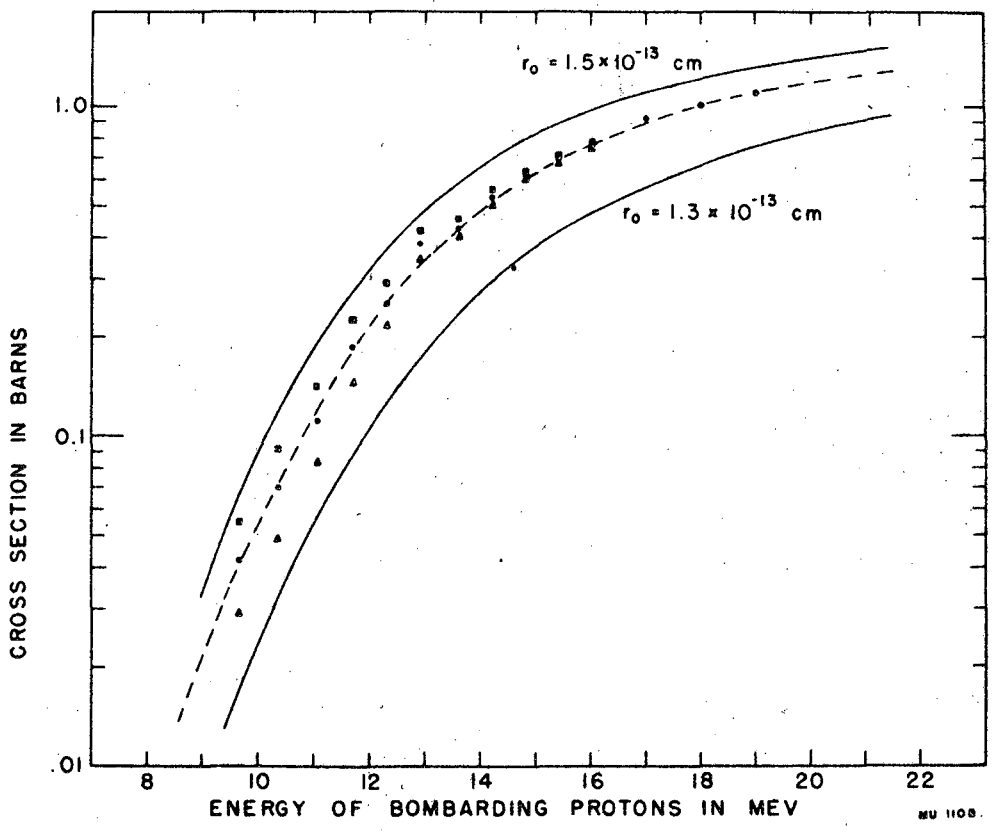

Fig. 18. This is the same as Fig. 17 except that the energy scale of the experimental points has been shifted by approximately 0.4 Mev.

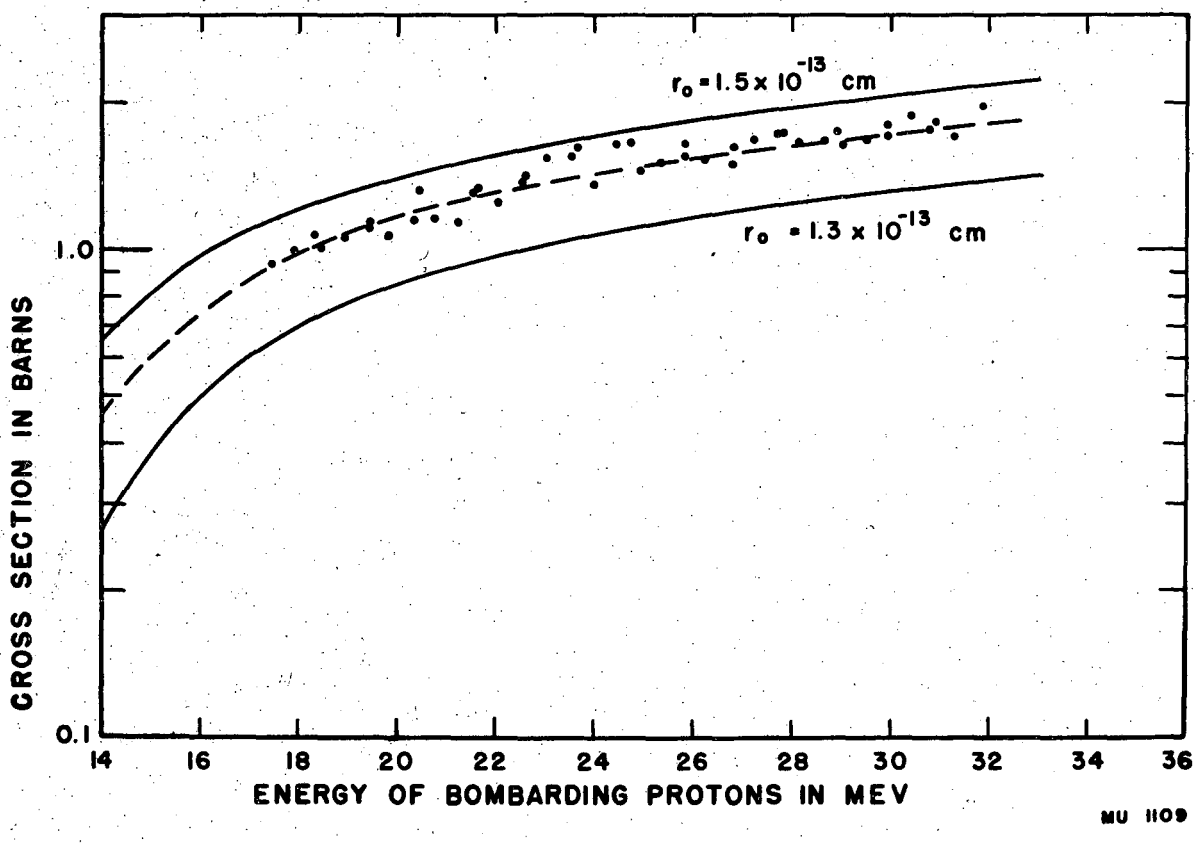

Fig. 19. Cross section plotted as a function of the energy of the bombarding protons. Theoretical values for the Bi + p compound nucleus cross section are shown by the solid and dashed curves. The points represent the sum of the experimental cross section values for the $Bi(p,n)Po^{209}$, the $Bi(p,2n)Po^{208}$, the $Bi(p,3n)Po^{207}$, and the $Bi(p,4n)Po^{206}$ reactions. The K-branching ratios for Po^{207} and Po^{206} have been assumed to be 1.4×10^{-4} and 4×10^{-2} respectively.

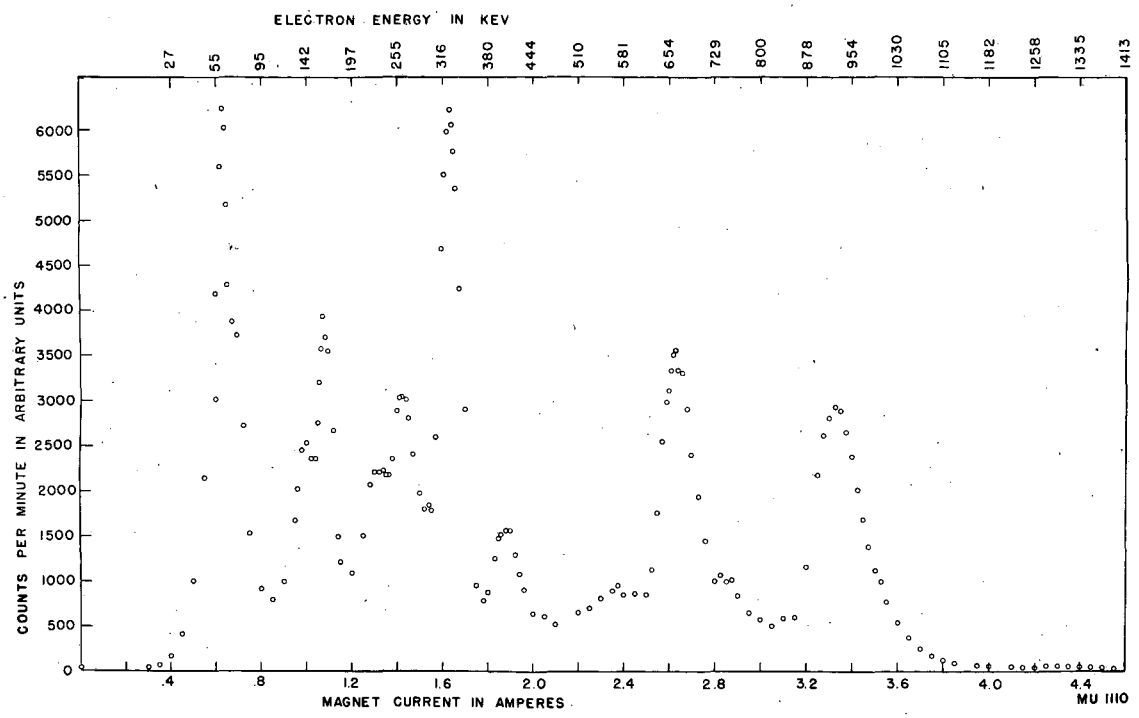

Fig. 20. Electron counting rate in arbitrary units plotted against magnet current and a corresponding energy scale for the electrons emitted by Po^{207}.

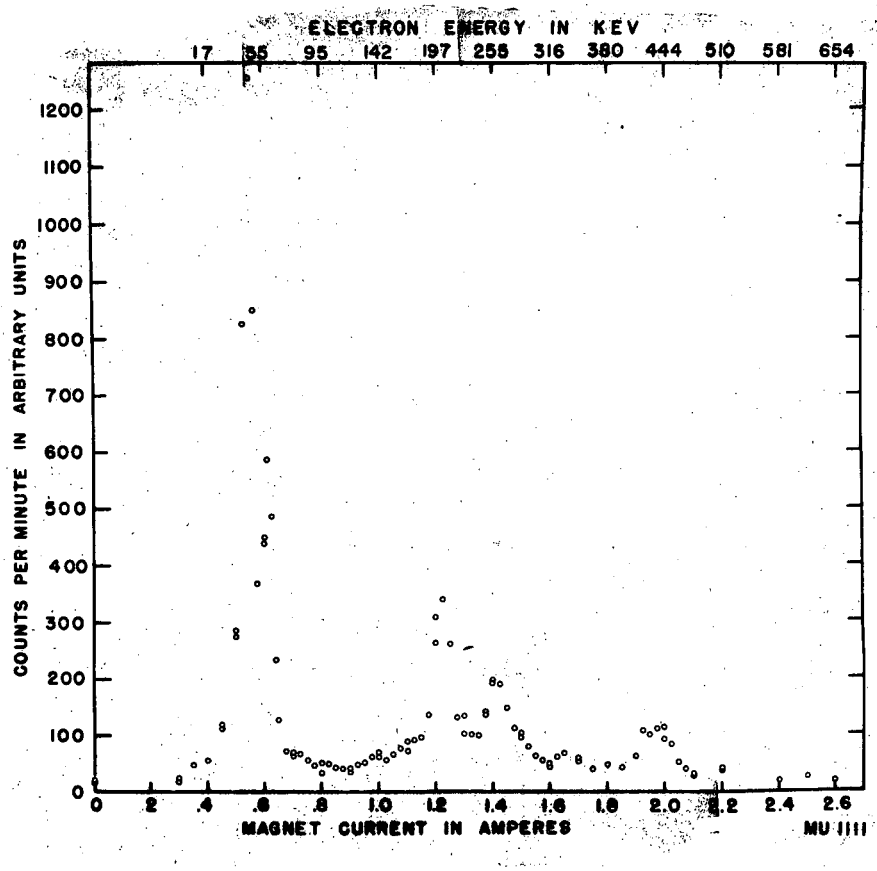

Fig. 21. Electron counting rate in arbitrary units plotted against magnet current and a corresponding energy scale for the electrons emitted by Po^{206}.

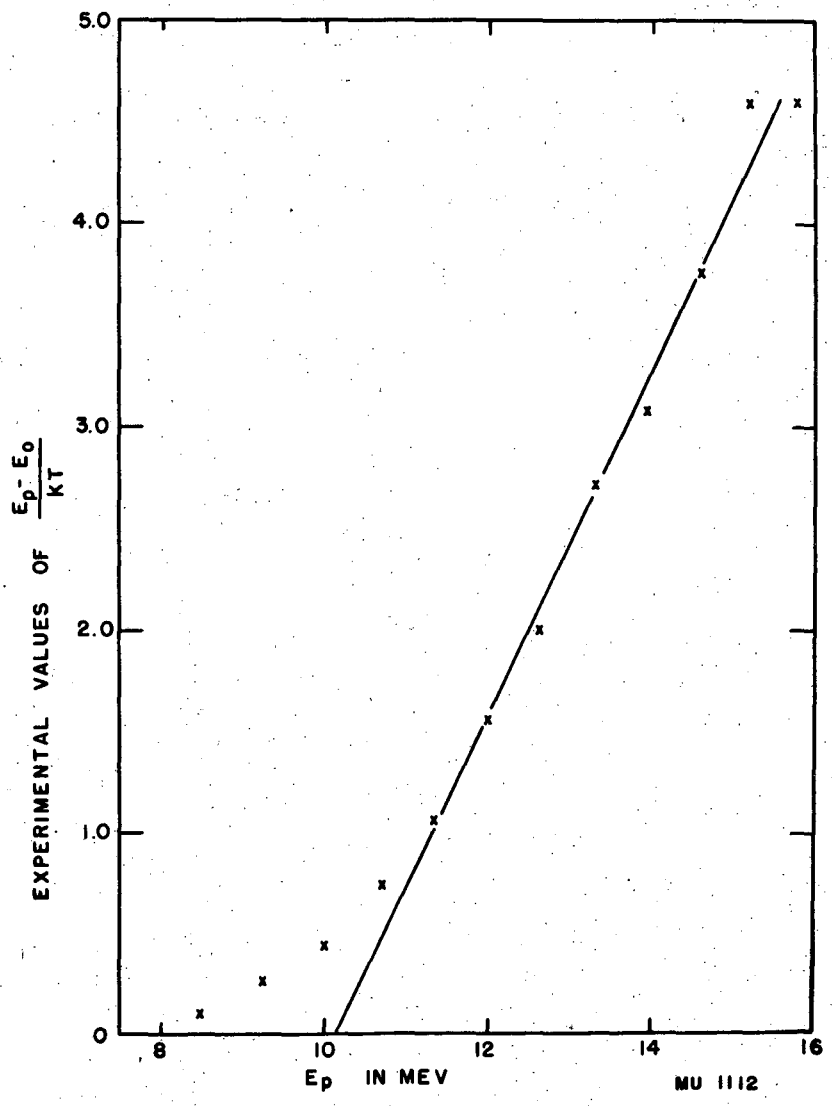

Fig. 22. Experimental values of the energy of the bombarding protons above the Bi(p,2n) threshold expressed in units of the nuclear temperature, kT, plotted against the energy of the bombarding protons.

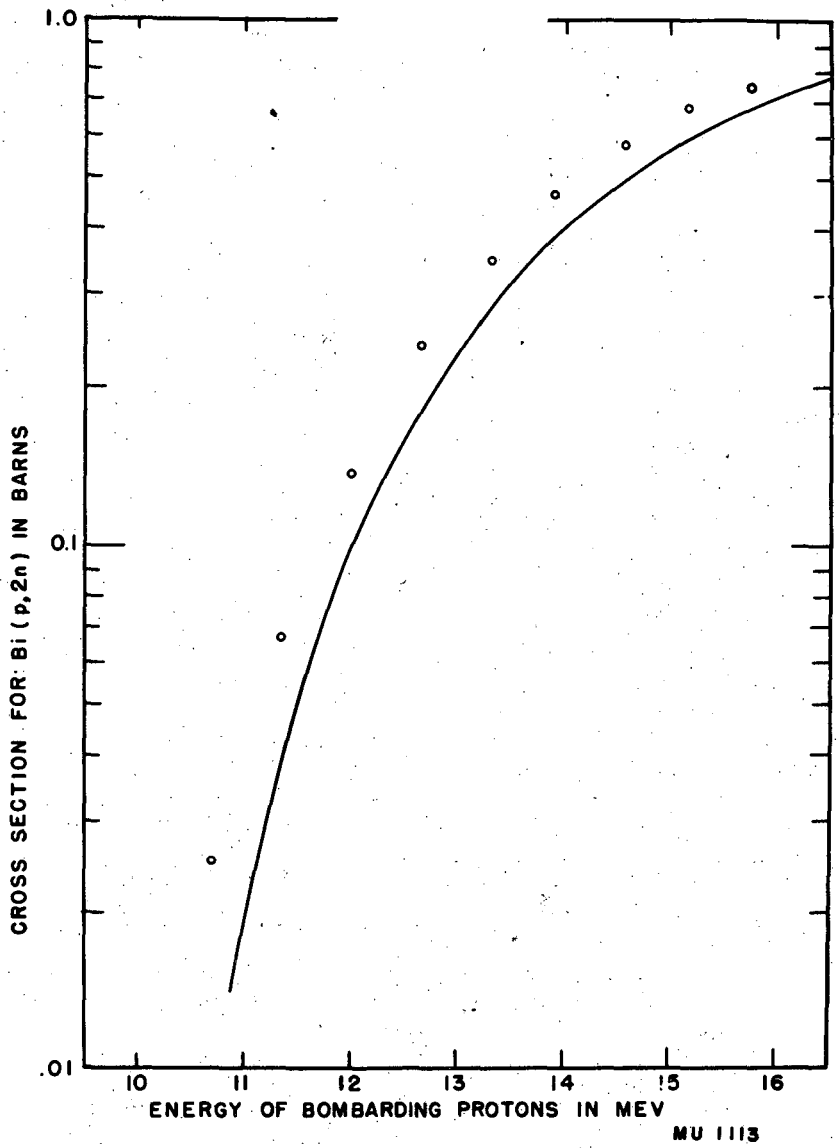

Fig. 23. Theoretical and experimental cross sections for the Bi(p,2n) reaction plotted versus the energy of the bombarding protons. The theoretical values are given by the solid curve and the points represent the experimental data.